Materials Advances

ROYAL SOCIETY OF CHEMISTRY

PAPER

View Article Online
View Journal | View Issue

Cite this: *Mater. Adv.*, 2025, 6, 2405

The role of dialdehyde kefiran as a crosslinking agent in chitosan/kefiran-based materials with "Henola" extracts: a biocompatible strategy in wound care†

Dorota Chelminiak-Dudkiewicz, *[a] Miloslav Machacek,[b] Jolanta Dlugaszewska,[c] Kinga Mylkie,[a] Aleksander Smolarkiewicz-Wyczachowski,[a] Magdalena Kozlikova,[b] Sebastian Druzynski,[d] Rafal Krygier [e] and Marta Ziegler-Borowska [a]

Due to the significant increase in patients struggling with wound treatment, the development of new natural wound dressings is now attracting much more attention. An important aspect that enhances these properties is the proper crosslinking of the materials. Therefore, in this study, we successfully produced films based on a mixture of chitosan and kefiran, crosslinked with kefiran dialdehyde. Our team obtained this crosslinker for the first time, and it is a safe alternative to standard agents such as glutaraldehyde. Moreover, to provide antimicrobial properties of the designed materials, we introduced an extract from the hemp variety "Henola" into the biopolymer matrix. Several analyses were performed to characterize the obtained films (such as FTIR-ATR, AFM, biodegradability, swelling rate, water vapor permeability, and mechanical properties). The biocompatibility of the films was tested using fibroblasts and erythrocytes, and their antimicrobial activity was examined against the bacteria and the fungus. The results showed that crosslinking with dialdehyde kefiran conferred strength and flexibility to the obtained films. Moreover, the film with the ethanol extract showed strong anti-inflammatory properties (86.4 ± 3.67%) and a strong inhibitory effect on the growth of *S. aureus* (the number of isolated cells was up to 5.7 log lower than that of the control). In addition, the materials do not exhibit hemolysis (≤5%) on contact with blood and are non-toxic to MRC-5 cells (after 24 hours, cell viability above 100%). Therefore, these films have promising potential for practical applications in wound dressing.

Received 11th January 2025,
Accepted 15th March 2025

DOI: 10.1039/d5ma00029g

rsc.li/materials-advances

Introduction

The skin is the body's protective barrier against environmental influences, microorganisms, and some harmful external agents. When the skin is injured (due to trauma, infection, or some disease process), the body tissue loses its integrity, creating a wound.[1,2] Once it happens, the body begins wound healing, which involves a complex physical, chemical, and cellular interaction, among which the stages of hemostasis, inflammation, proliferation, and remodeling are distinguished.[3,4] Based on understanding the physiological process of wound healing, the optimal dressing should be non-toxic, flexible, durable, moisturizing, and breathable, absorb exudate, have anti-inflammatory, antibacterial, and antioxidant properties, and promote cell proliferation and wound healing.[5–7]

As a result, the use of polysaccharides as a matrix for dressings has received increasing attention in recent years. Compared to numerous synthetic polymers, natural macromolecules represented by polysaccharides (such as chitosan, collagen, and alginate) show a higher affinity for mammalian tissues.[8–12] Chitosan (CS) is usually derived from shrimp shells and other sea crustaceans. This polysaccharide (known for stimulating fibroblast activity, cytokine production, and hydrophilicity) will promote wound healing and reduce scarring.[13,14] However, materials based on chitosan exhibit limited flexibility and insufficient barrier properties[15,16] For example, R. Adamski *et al.*[17] found that chitosan-based scaffolds have low tensile strength and fracture stiffness. In addition, B. Shi showed that

[a] *Department of Biomedical Chemistry and Polymer Science, Faculty of Chemistry, Nicolaus Copernicus University in Torun, Gagarina 7, 87-100 Torun, Poland. E-mail: dorotachd@umk.pl*
[b] *Department of Biochemical Sciences, Faculty of Pharmacy in Hradec Kralove, Charles University in Prague, Akademika Heyrovskeho 1203, 500 05 Hradec Kralove, Czech Republic*
[c] *Department of Genetics and Pharmaceutical Microbiology, Poznan University of Medical Sciences, Rokietnicka 3, 60-806 Poznan, Poland*
[d] *Department of Chemical Technology, Faculty of Chemistry, Nicolaus Copernicus University in Torun, Gagarina 7, 87-100 Torun, Poland*
[e] *NZOZ Gemini outpatient clinic, Os. Sloneczne 2, 62-571 Zychlin, Poland*

† Electronic supplementary information (ESI) available. See DOI: https://doi.org/10.1039/d5ma00029g

chitosan films have relatively high water vapor permeability, which results in limited moisture barrier effectiveness (8.07×10^{-13}–4.55×10^{-10} g m^{-1} s^{-1} Pa^{-1}).[18] Combining CS with another polysaccharide may improve some of its physicochemical and biological properties, thus showing great potential in wound healing. Kefiran (Kef) is worth paying attention. It is an exopolysaccharide composed of glucose and galactose obtained from microorganisms in kefir grains. It is synthesized by a few *Lactobacillus* species, *e.g.*, *L. kefiranofaciens*, *L. kefirgranum*, *L. parakefir*, *L. kefir*, *L. delbrueckii* subsp. *Bulgaricus*.[19,20] Kef exhibits antibacterial and antifungal properties,[21] which makes it suitable for wound dressing materials. This polysaccharide is combined with other polymers (mainly synthetic) for medical applications. In particular, Kef has been incorporated into composite films with polymers such as poly(vinyl alcohol) and poly(vinyl pyrrolidone).[22] These composites have been tested for their potential in biomedical fields, including tissue engineering and regenerative medicine. In addition, kefiran was chemically modified by reacting this polysaccharide with methacrylic anhydride for tissue engineering applications.[23] Some physicochemical properties can be improved by crosslinking. The most used crosslinking agent is glutaraldehyde, which is cytotoxic, thus limiting its use in biomedical applications. Doustdar *et al.*[24] described the effect of calcium chloride and glutaraldehyde (GA) on the properties of the obtained scaffolds based on chitosan/cellulose nanocrystals. They found that although the GA-containing scaffolds were biocompatible, GA had a negative effect on the cell proliferation ability of scaffolds, which is related to the cytotoxicity of GA itself. The cytotoxicity of glutaraldehyde was also confirmed in another study, in which collagen–chitosan scaffolds cross-linked with GA were obtained. This material showed a decrease in cell viability of L929 fibroblasts (up to 50%).[25]

In addition to glutaraldehyde, glyoxal is also known. It is an effective crosslinking agent for biomaterials, but its toxicity depends on the concentration and method of application. Studies have shown that glyoxal was cytotoxic to hepatocytes at higher concentrations, which is attributed to glutathione depletion, oxidative stress, and mitochondrial toxicity.[26] Another example is EDC/NHS (1-ethyl-3-(3-dimethylaminopropyl)carbodiimide/*N*-hydroxysuccinimide). Although it is widely used due to its low cytotoxicity compared to other crosslinking agents (such as glutaraldehyde), some studies suggest that byproducts of EDC reactions may exhibit some toxicity.[27,28] Therefore, the present study prepared a synthesis for non-toxic dialdehyde kefiran (DKef). DKef distinguishes itself from conventional crosslinking agents by combining high chemical reactivity with favorable biocompatibility properties. As a derivative of the natural polysaccharide kefiran, it is fully biodegradable, eliminating the risk of accumulating toxic degradation products. Unlike glyoxal, it does not exhibit strong cytotoxic properties and does not induce oxidative stress. In addition, unlike EDC/NHS, it does not require aggressive post-crosslinking purification, simplifying the biomaterials preparation procedure. Notably, this compound was used as a crosslinker for the first time.

To enhance the medicinal properties of designed dressing materials, natural plant extracts that improve wound healing properties without causing toxicity have gained increasing interest in recent years.[29,30] Many studies are based on chitosan with plant extracts. An example is the use of *Centella asiatica* extract.[31] Combining chitosan with this extract has shown synergistic effects, including the ability to inhibit hyaluronidase and antimicrobial activity, which promotes regenerative processes in wound healing.[32] Another example is the use of *Catharanthus roseus*, a plant that exhibits antioxidant, anti-inflammatory, and anticancer activities. A chitosan/PVA biocomposite doped with MgO and enriched with this extract has been shown to increase the biological activity of the material significantly.[33] Saied *et al.*[34] performed a study on combining chitosan with apricot kernel (*Prunus armeniaca*) seed extract. Incorporating this extract into chitosan films significantly increases their antioxidant and antimicrobial properties, making them potential materials for biomedical applications. Among several plants, many beneficial properties are possessed by *Cannabis sativa* L. hemp, which contains cannabinoids, terpenes, flavonoids, vitamins, and minerals. The literature shows that cannabis flowers exhibit analgesic, antioxidant, antibacterial, anti-inflammatory, regenerative, and blood-clotting properties.[13,35] According to the Polish National List of Agricultural Plant Varieties,[36] 11 different hemp varieties are grown in Poland. All types contain less than 0.2% of the psychoactive tetrahydrocannabinol (THC). Our study used the ''Henola'' variety, which has only been tested for food[37] and bioethanol production.[38] ''Henola'' is an oil hemp variety with at least twice the yield of other types available on the market, low growth (up to about 2 m), and a 3-week shorter growing season. ''Henola'' is registered with the National List of Agricultural Plant Varieties under number R2908 and has received approval from the Colorado Department of Agriculture, USA. Henola seeds comprise approximately 75% polyunsaturated fatty acids (PUFAs), with linoleic acid (55%) and α-linolenic acid (13–15%), yielding an optimal omega-6 to omega-3 ratio of 3 : 1. Additionally, they contain monounsaturated oleic acid (12–15%) and a lower proportion of saturated fatty acids (10–11%).[39,40] Beyond its lipid composition, ''Henola'' is a valuable source of high-quality protein, encompassing all essential amino acids. Among these, leucine is the most abundant, followed by valine and isoleucine, highlighting its potential as a plant-based protein alternative. Moreover, its seeds supply essential minerals, including calcium, magnesium, potassium, iron, manganese, copper, and zinc.[41] Concerning its cannabinoid profile, ''Henola'' complies with industrial hemp regulations by maintaining a THC content below 0.3% while maintaining bioactive potential. In addition to cannabidiol (CBD, ~0.7%), it also contains cannabigerol (CBG), another non-psychoactive cannabinoid with therapeutic promise.[42]

In this work, a dialdehyde kefiran not previously described in the literature was obtained and then used as a crosslinking agent for chitosan–kefiran films enriched with two ''Henola'' extracts (aqueous and ethanol). The materials were characterized entirely for their potential use as dressing materials

(including physicochemical and biological properties). The results show that the designed films meet most of the characteristics required for an ''ideal'' dressing material.

Experimental section

Materials

Chitosan (CAS number: 448869; low-molecular-weight, DP: 50 000–190 000 Da (based on viscosity), DDA: 79%), glycerin, ethanol (96.6%), sodium periodate, diiodomethane (pure for analysis), phosphate buffer saline (PBS) (pH 7.4), diclofenac sodium, human serum albumin (HSA), bovine serum albumin (BSA), fibrinogen, hen egg white lysozyme, and 2,2-diphenyl-1-picrylhydrazyl radical (DPPH) were purchased from Sigma-Aldrich (Merck KGaA, Darmstadt, Germany). Acetic acid was supplied by Avantor Materials Poland S.A. (POCH, Gliwice, Poland). Kefir grains were obtained from local culinary store. The ''Henola'' hemp (*Hen*) variety came from a local grower (plant sowed April 21, harvested July 2023 in 1.5 m height from soil class V pH 4–5, dried naturally (in the attic)).

Materials for the antimicrobial tests: *Staphylococcus aureus* (ATCC 29213), *Pseudomonas aeruginosa* (ATCC 27853), and *Candida albicans* ATCC 10231. Brain Heart Infusion Broth (Oxoid, UK), Tryptone Soya Agar (Oxoid, UK), Sabouraud dextrose broth (Merck KgaA, Germany), Malt extract agar (Merck KgaA, Germany), Sodium chloride (Avantor Performance Materials Poland S.A., Poland).

Materials for biocompatibility tests: MRC-5 (CCL-171) from American Type Culture Collection (ATCC; Manassas, Virginia, USA). Cultivation flasks and flat-bottom plates for cell cultures were purchased from TPP (Trasadingen, Switzerland). Round bottom 96-well plates were manufactured by Gama (České Budějovice, Czech Republic), microcentrifuge tubes and pipette tips by Eppendorf (Hamburg, Germany). Cell culture was maintained in Dulbecco's Modified Eagle Medium (Capricorn Scientific, Ebsdorfergrund, Germany) supplemented with 10 vol% fetal bovine serum, 10 mM HEPES buffer, 4 mM L-alanyl-L-glutamine, 1 × penicillin/streptomycin solution (Capricorn) and 1 × MEM Non-essential amino acid solution (Sigma-Aldrich). Purified water was prepared using Milli-Q Ultrapure Water System (Merck KGaA, Darmstadt, Germany).

Isolation and characterization of kefiran (Kef)

The kefir grains were stored in skimmed milk at room temperature (rt) for seven days. The milk was changed daily to maintain the viability of the grains. Kefiran from kefir grains was isolated according to the method described by Piermaria *et al.*[43] Kefir grains (10 g) were treated with distilled water (100 mL) and stirred at 100 °C for 1 h with a magnetic stirrer. Then, the mixture was centrifuged at 10 000 × *g* for 20 min at 20 °C. Ethanol (60 mL) was added to the supernatant to precipitate the kefiran. The polysaccharide was placed in the freezer at −24 °C for 12 h, then centrifuged at 10 000 × *g* and 4 °C. The mixture was re-dissolved in hot distilled water, and the precipitation was repeated with ethanol. Finally, the mixture was frozen at −24 °C and freeze-dried for 48 h.

The total carbohydrate content was defined using the phenol–sulphuric acid colorimetric assay, with D-glucose as the calibration standard and absorbance measured at 490 nm.[44] Protein content was evaluated employing the Bradford method, utilizing bovine serum albumin (BSA) as the reference standard for calibration.[45]

Preparation and characterization of dialdehyde kefiran (DKef)

Freshly isolated kefiran (0.3 g) was dissolved in boiling water (30 mL) under continuous magnetic stirring (100 °C, 2 h, 550 rpm). The oxidation was carried out by adding a sodium periodate solution (0.7 M) at an oxidant-to-kefiran weight ratio of 1 : 1. The reaction mixture was stirred at 400 rpm and maintained at 40 °C without light for 3 h. After cooling to rt, acetone (60 mL) was slowly added while maintaining constant stirring (600 rpm) until dialdehyde kefiran (DKef) precipitation was observed (20 min). The precipitate was collected by filtration, washed thrice with deionized water, and dried at rt for 24 h.

Total carbohydrate content was determined using a phenolic–sulfuric acid colorimetric test, and protein content was assessed using the Bradford method for unmodified kefiran.

Determination of the contents of the aldehyde groups

The content of aldehyde groups in the dialdehyde kefiran sample was determined according to the procedure's previous description.[14] The freshly obtained DKef sample (0.15 g) was dissolved in distilled water (2 mL), and sodium hydroxide (10 mL, 0.20 M) was added. Next, the mixture was heated in a water bath at 70 °C for 2 minutes and then cooled with cold water for 1 minute. Then, hydrochloric acid (10 mL, 0.20 M) and phenolphthalein (1% w/w, 1 mL) were added. The obtained solution was titrated with sodium hydroxide (0.2 M). The percentage of dialdehyde units was given by the equation:

$$\text{Content of aldehyde groups } (\%) = \frac{C_1V_1 - C_2V_2}{m/M} \times 100\%$$

where: C_1 and V_1 are the concentration and volume of NaOH solution, C_2 and V_2 are the concentration and volume of HCl solution, respectively; m – mass of the sample (g), M – molecular weight of the repeated unit in dialdehyde kefiran (M = 344.31 g mol^{-1}).

Dynamic light scattering (DLS)—particle size analysis

The size distrubution of the Kef and DKef was measured with a Malvern Nano Zetasizer ZS90 instrument (Malvern, UK). Measurements were performed using a detection angle at 25°. The samples were diluted with deionized water.

Attenuated total reflectance spectroscopy (ATR-FTIR)

Structures of the kefiran and dialdehyde kefiran were characterized by the Attenuated Total Reflectance Fourier Transform Infrared (ATR-FTIR) spectroscopy using Spectrum Two™ (PerkinElmer, Waltham, MA, USA) spectrometer equipped with

the diamond crystal. Spectrum was recorded in the 4000 to 450 cm^{-1} range at a resolution of 4 cm^{-1}, and 64 scans. After recording the spectrum, the baseline, normalization, and ATR corrections were made.

Scanning electron microscopy (SEM)

The morphology of the Kef and DKef was studied with a scanning electron microscope (1430 VP LEO Electron Microscopy Ltd).

^{13}C NMR analysis

^{13}C NMR spectra of Kef and DKef were recorded with a Bruker Avance III 700 MHz solid-state NMR spectrometer at 294 K.

Plant material and extraction

The Hen was collected from its natural state in July 2023 in Poland, at a height of 1.5 m, from class V soil with a pH of 4–5, from a crop owned by Dr Rafal Krygier. Plants were randomly selected from different, close locations and then dried in the attic to a constant weight.

Freshly harvested Hen was tested for elements using the flame atomic absorption spectrometry (FAAS) technique and ICP technique. Preparation of samples of the tested material for FAAS analysis involved classic wet mineralization. The dried Hen was subjected to mechanical homogenization. Next, three samples of approximately 5 g were weighed with an accuracy of ±0.0001 g in Kjeldahl flasks. To each sample, 30 cm^3 of 65% nitric acid (V) was added and left for 24 hours at room temperature (rt). Then, the samples were heated until the organic matter was completely decomposed, and the excess acid was reduced (to approximately 5 cm^3). After that, 10 cm^3 of 30% hydrogen peroxide was added, and heating was continued until the excess of peroxide was wholly decomposed. After cooling, the samples were quantitatively transferred to 50 cm^3 volumetric flasks and analyzed.

The dried raw Hen was extracted using the Soxhlet technique. Two types of extracts were prepared. In each case, fifteen grams of dried hemp was placed in a Soxhlet apparatus. Extraction was performed with 250 mL ethanol (96.6% v/v) or 250 mL water for six hours at rt. After extraction, the suspension was filtered and concentrated using a rotary evaporator at 40 °C. The samples were stored in the dark at 4 °C.

Preparation of chitosan/kefiran films with plant extracts cross-linked with dialdehyde kefiran (CS/Kef/WE and CS/Kef/EE)

First, two separate polysaccharide solutions were prepared. To do this, chitosan (CS) (0.2 g) was dissolved in acetic acid (C = 1%, 20 mL), and kefiran (Kef) (0.23 g) was dissolved in boiling distilled water (12 mL). The final concentration of chitosan is 1% w/w, and the concentration of kefiran is 2% w/w. The choice of these values was based on previous studies and preliminary experiments. It was shown that film-forming solutions containing 2% kefiran could be easily removed from the wafer surface. Next, these two solutions were mixed, and dialdehyde kefiran (15% by weight of chitosan or kefiran) was added. The mixture was stirred for 1 h at rt using a magnetic stirrer. Then, a drop of glycerin and water (WE) or ethanol (EE) and plant extract (5 mL) were added, and stirring was continued for one hour. Finally, the obtained mixtures were poured into Petri dishes and left to evaporate the solvent at rt for 48 h. The following terms are used further in the manuscript: chitosan–kefiran film with aqueous plant extract (CS/Kef/WE) and chitosan–kefiran film with ethanol plant extract (CS/Kef/EE).

Physicochemical properties of the CS/Kef/WE and CS/Kef/EE

Attenuated total reflectance spectroscopy (ATR-FTIR). Structures of the obtained films were characterized by the Attenuated Total Reflectance Fourier Transform Infrared (ATR-FTIR) spectroscopy using Spectrum Two™ (PerkinElmer, Waltham, MA, USA) spectrometer equipped with the diamond crystal. Spectra were recorded in the 4000 to 450 cm^{-1} range at a resolution of 4 cm^{-1}, and 64 scans. After recording the spectra, the baseline, normalization, and ATR corrections were made.

Atomic force microscopy (AFM). The topography of the films was examined by atomic force microscopy (AFM) and analyzed using NanoScope Analysis software. Roughness parameters (root mean square (R_q) and arithmetic mean (R_a)) were calculated for the 5 × 5 μm^2 scanning area.

Thermogravimetric analysis (TGA). Thermal gravimetric analysis of the obtained films was conducted on a TA Instruments (SDT 2960 Simultaneous DSC-TGA thermogravimetric analyzer) at a 10 °C min^{-1} heating rate in the range from ambient to 600 °C in the atmosphere of nitrogen.

Contact angle measurement. The contact angle (θ) of CS/Kef, CS/Kef/WE, and CS/Kef/EE films was performed at 22 °C by the sessile drop method using an OCA 15 EC goniometer (SpectroLab, Poland). Two types of liquid with different polarity were used: glycerin and diiodomethane. Surface free energy (γ_s) and its polar (γ_s^p) and dispersive (γ_s^d) components were calculated by the standard Owens–Wendt theory.[46] At least three measurements were conducted to assess each sample.

Cross-linking degree of the CS/Kef, CS/Kef/WE, and CS/Kef/EE

According to literature reports, an extraction method has been used to determine the degree of cross-linking of CS/Kef, CS/Kef/WE, and CS/Kef/EE films.[47] A square (1 cm × 1 cm) was cut from the film and weighed (m_1). Next, such prepared sample was placed in a flask containing acetic acid (40 mL, C = 1%) and extracted at 70 °C for 24 hours. The insoluble residue was filtered, dried at 60 °C in a vacuum dryer for 24 h, and then re-weighed (m_2). The cross-linking degree (C, %) of the CS/Kef, CS/Kef/WE, and CS/Kef/EE films can be expressed as:

$$C\ (\%) = m_2/m_1 \times 100\% \quad (1)$$

Mechanical properties of the CS/Kef, CS/Kef/WE, and CS/Kef/EE

The mechanical properties of CS/Kef, CS/Kef/WE and CS/Kef/EE films were tested at rt by the EZ-Test E2-LX Shimadzu texture analyzer (Shimadzu, Kyoto, Japan). Three sample strips (50 mm in length and 4.5 mm in width) of CS/Kef, CS/Kef/WE, and CS/Kef/EE films were cut and clamped between pneumatic grips.

The studies were conducted at an extension rate of 20 mm min^{-1}, and each measurement was repeated three times.

Swelling analysis

The swelling ratio of CS/Kef, CS/Kef/WE, and CS/Kef/EE were calculated using the gravimetric method as previously described.[4] Samples of known weight (m_1) were immersed in a PBS solution (4 mL) of pH 5.6 and 7.4 at 37 °C. After a specified time, the samples were removed, wiped from excess water, and weighed (m_2). The experiment was conducted in triplicate. The swelling rate was calculated using the following formula:

$$\text{Swelling rate (\%)} = (m_2 - m_1)/m_1 \times 100\% \quad (2)$$

Biodegradation analysis

The biodegradability of Cs/Kef, CS/Kef/WE, and CS/Kef/EE films was determined by monitoring their weight changes for 14 days. Films of known mass (m_0) were incubated in PBS solution (pH = 7.4, 37 °C) containing lysozyme (0.5 mg mL^{-1}). Lysozyme was added to PBS to simulate enzymatic degradation conditions in the body, as it is a key enzyme that degrades polysaccharides in body fluids. After each day, the films were removed from the solution, washed with deionized water, freeze-dried, and re-weighed (m). The biodegradability of the films was calculated using the following formula:

$$\text{Biodegradation (\%)} = (m_0 - m)/m_0 \times 100\% \quad (3)$$

The water vapor transmission rate (WVTR)

First, calcium chloride, functioning as a desiccant, was dried at 100 °C for 24 h. Next, the desiccant was poured into a plastic box (diameter 40 mm). The obtained films were cut into round shapes and then placed on the top surfaces of the box. The boxes were sealed tightly, while the open boxes with the desiccant were left as control samples. After a particular time, the film was removed, and the mass of desiccant with adsorbed water was measured. The WVTR of the films was calculated using the following formula:

$$\text{WVTR (g } m^{-2} \text{ } h^{-1}) = (\Delta w/\Delta t)/A \quad (4)$$

where ($\Delta w/\Delta t$) denoted the slope of the plot and A denoted the effective transfer area.

Oxygen permeability

Boiling distilled water (200 mL) was added to the bottle. The tested films were attached to the top of the bottle. The positive control was the open bottle, while the negative control was the closed bottle. All samples were left under ambient conditions for 24 hours. The results were expressed as the amount of dissolved oxygen (mg mL^{-1}). The experiment was conducted three times.

Antioxidant activity

The DPPH radical scavenging assay was used to measure the radical scavenging activity of the films. Ascorbic acid, which has high antioxidant activity, was used as a model compound. In short, freshly prepared DPPH reagent (1.0 mM in ethanol) was added to ascorbic acid and tested films (30 μL). The sample was incubated at rt for 30 minutes in the dark. Then, its absorbance (A_F) at 517 nm was recorded against the blank (A_0) using a UV-1800 spectrophotometer (Shimadzu, Japan). The experiment was conducted three times. The DPPH radical scavenging was calculated using the following formula:

$$\text{DPPH scavenging (\%)} = (A_0 - A_F)/A_0 \times 100\% \quad (5)$$

Anti-inflammatory activity

The anti-inflammatory activity of the CS/Kef, CS/Kef/WE, and CS/Kef/EE films was determined was determined by inhibiting the denaturation of bovine serum albumin (BSA) by the obtained materials.[48] BSA solution (5 mL, 5%) was mixed with film (1 cm diameter). The mixtures were incubated at 37 °C for 15 minutes (200 rpm min^{-1}), then transferred to a water bath and set at 70 °C for 5 minutes to cause protein denaturation. Diclofenac sodium salt was used as a model compound. The absorbance of the obtained blends and the model solution was measured spectrophotometrically at 278 nm. Measurements were performed for different concentrations (10–500 μg mL^{-1}). The experiment was conducted three times. The percentage of inhibition of denaturation was calculated using the following formula:

$$\text{Inhibition (\%)} = (A_s - A_c)/A_s \times 100\% \quad (6)$$

where A_c is the absorbance of the control and A_s is the absorbance of sample.

Protein adsorption

The fluorescence method determined the adsorption of proteins on the CS/Kef, CS/Kef/WE, and CS/Kef/EE films, according to the procedure described in our previous work.[49] We used two proteins to test the interaction: human serum albumin (HSA) and fibrinogen (Fb). Protein adsorption of the obtained films was determined using a spectrofluorometer. Foremost, the solution of HSA (6.24 μM) and Fb (3.78 μM) in PBS (pH = 7.4; 50 mM) was prepared. The film's 4 cm^2 area was then immersed in four milliliters of freshly prepared HSA or Fb solution and incubated at 36 °C and 600 rpm. Fluorescence spectra were recorded at various time intervals at 25 °C, ranging from 290 to 400 nm and 300 to 500 nm for HSA and Fb, respectively, with an excitation wavelength of 280 nm, using a Jasco FP-8300 spectrofluorometer (Jasco, Tokyo, Japan). The spectral registration range was 285–400 nm, scanning speed 100 nm min^{-1}, and Em/Ex bandwidth 2.5 nm/5 nm.

Antimicrobial properties assay

Preparation of microbial inoculum. The antimicrobial properties of the CS/Kef, CS/Kef/WE, and CS/Kef/EE films were tested against standard strains of a Gram-negative bacterium – *Pseudomonas aeruginosa* (*P. aeruginosa*), a Gram-positive bacterium – *Staphylococcus aureus* (*S. aureus*), and yeast-like fungus – *Candida albicans* (*C. albicans*). Bacterial cultures were grown in Brain

Heart Infusion broth (BHI, Oxoid, UK) at 36 °C ± 1 °C for 18 h, and yeast cultures were grown in Sabouraud dextrose broth (SDB, Merck KgaA, Germany) at 36 ± 1 °C for 24 h. After incubation, the microorganisms were harvested by centrifugation (3000 rpm for 15 min), re-suspended, and diluted in a suitable liquid medium (*P. aeruginosa*, *S. aureus* – BHI; *C. albicans* – SDB) to obtain a final suspension density about 10^6–10^7 CFU per mL.

Time-kill curve assay

Time-kill curve studies were carried out as previously described by culturing bacterial and fungal strains in a suitable liquid medium (bacteria – BHI, fungi – SDB) in the presence of tested films (10 mg mL^{-1}). The initial number of microbial cells was about 10^5–10^6 CFU per mL, and the final volume of the sample was 1000 μL. The growth control tube was filled with medium only. Samples were incubated at 36 ± 1 °C. On 0 h, four h, eight h, 12 h, 16 h, 20 h, and 24 h incubation, the numbers of microbial cells were determined by the plate count method. The lower limit of detectable colony count was 20 CFU per mL. The time-killing curves were analyzed by plotting the log 10 CFU per mL against the time. Experiments were performed in triplicates on three different days.

Biocompatibility of the films

The *in vitro* biocompatibility of CS/Kef, CS/Kef/WE, and CS/Kef/EE films was evaluated by exposing MRC-5 cell to the films. Squares (0.59 × 0.59 cm, which correspond to the growth surface of the 96 well plate) were cut from the films, placed into sterile 96-well plates (TPP, Switzerland) and covered with 300 μL of sterile 0.1 M NaOH for 30 min to neutralize remnants of acetic acid. Subsequently, NaOH was removed, and samples were washed two times (300 μL, 30 min each) with sterile PBS. Buffer was removed and 300 μL ultrapure sterile water was added for 30 min – this step was repeated once. The same procedure was also applied to empty wells. Samples were dried in a sterile environment of a laminar flow box overnight and UV sterilized for 20 min. Subsequently, suspension of MRC-5 cells (100 000 cells per well in 200 μL) was added to each well and cell cultures were incubated with materials for 24 or 72 hours prior the assessment of cellular viability. Shortly, 50 μL of medium was removed from the cells and 50 μL of a fresh cell culture medium containing 20 vol% Almar Blue solution (Invitrogen, Thermo Fisher Scientific, Waltham, MA, USA) was added (5 vol% final concentration) for 2 h. Fluorescence (λ_{ex} = 560 nm, λ_{em} = 590 nm) was measured using Tecan Infinite 200 M plate reader (Tecan Group Ltd, Männedorf, Switzerland). Cells treated with lethal dose of hydrogen peroxide were used for a background subtraction. Results are expressed as % of untreated cells (100%).

Hemolysis assay

The *ex vivo* hemolytic activity of CS/Kef, CS/Kef/WE, and CS/Kef/EE films was tested on human red blood cells from an anonymous donor (Approval of the Ethical Committee of the Faculty of Pharmacy in Hradec Králové, Charles University no. UKFaF/46675/2023). Squares (1 cm^2) were cut from the films, placed into sterile 24-well plates (TPP, Trasadingen, Switzerland). Whole washing procedure was conducted as described above (Section 1.15 Biocompatibility of the films) with one difference – 1 mL of each washing fluid (NaOH, PBS, water) was used instead of 300 μL.

Venous blood was collected from anonymous donor using BD Vacutainer® system (Becton, Dickinson and Company, Franklin Lakes, NJ, USA) to EDTA-containing tubes and processed immediately after collection. After 10 min centrifugation (750 × *g*), plasma was replaced with the same amount of PBS, and centrifugation tubes were mixed by gentle inverting. Centrifugation and washing step was repeated three more times. Purified erythrocytes (RBCs) were diluted by PBS (25 mL of RBC and 75 mL of PBS), gently mixed and 1 mL of purified diluted RBCs was added to each sample in 24-well plate. For positive control, purified RBCs were diluted using ultrapure water instead of PBS. After 2 h incubation, each sample was gently resuspended, 200 μL of RBC suspension was transferred to round-bottom 96-well plates (Gama, České Budějovice, Czech Republic) and centrifuged for 10 min (750 × *g*). Supernatant (100 μL) was transferred to flat-bottom 96-well plates (TPP) and absorbance (540 nm) was measured using Tecan Infinite 200 M plate reader. Results are expressed as a % of positive control (100% hemolysis).

Statistical analysis

Statistical analysis was conducted in one-way analyses of variance (ANOVAs) followed by Dunnett test with GraphPad Prism version 6.0 (GraphPad Software, San Diego, CA, USA). Data are presented as means ± SDs. A *p*-value of <0.05 was considered statistically significant ($P^* < 0.05$, $p^{**} < 0.01$ and $p^{***} < 0.001$).

Results and discussion

Characterization of the kefiran (Kef) and dialdehyde kefiran (DKef)

The purified kefiran exhibited no detectable response in the Bradford assay, and no absorption peaks were observed in the UV spectrum at 280 or 260 nm, confirming the absence of protein contamination. The total carbohydrate content of kefiran was quantified as 98.12% ± 1.25% using the phenol–sulphuric acid method. These results are consistent with previous studies that reported high-purity kefiran obtained using the same isolation method.[43,44,50]

Dialdehyde kefiran (DKef) was obtained by the oxidation process of hydroxyl groups of kefiran using sodium periodate and the structure is shown in Fig. 1b. Notably, the reaction process is not complicated because, after adding acetone, the dialdehyde product precipitates out of the reaction mixture. The aldehyde group amount was 89%. In line with our findings, other works have reported comparable outcomes by oxidizing various polysaccharides. For example, a study by Keshk *et al.*[51] obtained dialdehyde starch with 91% aldehyde content; however, the reaction time (24 h) was much longer than in this

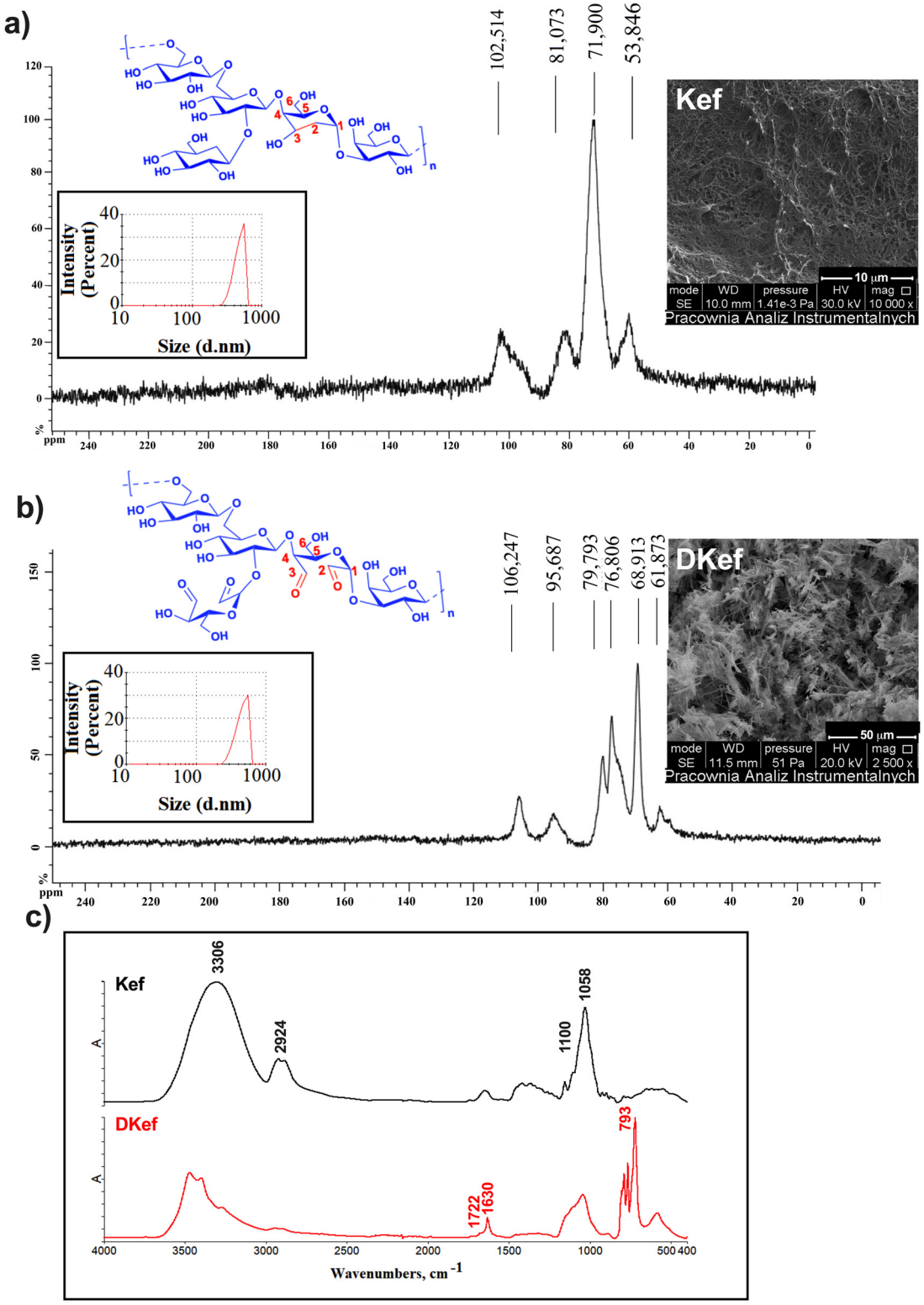

Fig. 1 Characterization of the native kefiran (Kef) and dialdehyde kefiran (DKef). The size distribution, SEM image, and ^{13}C NMR spectra of the (a) Kef and (b) DKef; (c) ATR-FTIR spectra of the Kef and DKef.

study. In addition, the molar ratio of starch glucose units to sodium periodate was 1 : 2.2, indicating a higher consumption of sodium periodate reagent than this experiment. In another study,[52] a dialdehyde alginate with 57% aldehyde content was obtained using a molar ratio of oxidizer/alginate of 1 : 1. This means that our study developed and used optimal and

repeatable conditions for obtaining dialdehyde kefiran. The phenol–sulfuric acid test showed a total carbohydrate content of 65 ± 1.12%, indicating a significant reduction compared to the Kef sample. This reduction is consistent with the oxidation of hydroxyl groups to aldehydes (89% degree of substitution) while retaining some of the original polysaccharide structure capable of reacting in the test. In addition, the Bradford assay did not show the presence of proteins in the DKef sample.

The primary analysis used standard methods such as ATR-FTIR and NMR spectroscopies, SEM, and DLS to confirm the modified polysaccharide. DLS analysis showed a hydrodynamic diameter of kefiran of 295 nm (Fig. 1a), with a Dispersity ($Đ$) of 0.292, indicating moderate homogeneity and no significant impurities in the sample. On the other hand, the average size of the dialdehyde kefiran (Fig. 1b) was 305 nm and $Đ$ = 0.502. The oxidation process reduced the ability of the molecules to form compact structures, which is characteristic of Kef, and allowed the formation of more flexible aggregates of larger size. The increased hydrodynamic particle diameter confirms that the structure of DKef retains its integrity despite the modification.

The morphology of the DKef was studied by scanning electron microscopy (Fig. 1b). SEM images of unmodified kefiran (Fig. 1a) showed loosely bound particles with irregular but porous surfaces. DKef took the form of elongated structures (Fig. 1b). Similar changes were observed with starch oxidation.[53,54]

The structure of the native and modified kefiran was characterized using ^{13}C NMR and ATR-FTIR spectra (Fig. 1c). In the ^{13}C NMR spectrum of the Kef, signals with a shift of 59.85 ppm (C6), a broad signal at 71.90 ppm (C2, C3, C5), and a signal at 81.07 ppm (C4) and 102.51 ppm (C1) are present. On the other hand, the spectrum of DKef lacks a signal between 170–190 ppm from the carbon of the aldehyde group. Signals from aldehyde groups are usually of low intensity, which can make them invisible in solid ^{13}C NMR spectra. In addition, according to the literature, the aldehydes formed are present as a hemiacetal and not as –CHO groups, as described for dialdehyde starch.[55]

In the ATR-FTIR spectrum of unmodified kefiran (Fig. 1c), characteristic absorption bands are present at 3306 cm^{-1} (attributed to hydroxyl groups), 2924 cm^{-1} (stretching vibration of C–H in the sugar ring), and in the 1100–1150 cm^{-1} region (C–O–C stretches). The spectrum is consistent with the literature data.[56] After kefiran oxidation, new bands appeared at 1722 cm^{-1} and 793 cm^{-1}, attributed to the aldehyde group's C═O stretching and C–H vibrations. In addition, a sharp band at 1630 cm^{-1} derived from the carbonyl group confirmed the success of the oxidation process. Significant changes were also observed in the vibration range of the C–O–C groups (1100–1150 cm^{-1}), indicating the effective modification of the glucoside rings caused by their opening and oxidation at the C2 and C3 positions.[57]

Plant material

Freshly harvested *Hen* was tested using the FAAS technique for elements content to assess its quality and safety. The results (Table 1) show that the studied plant material may have some potential as a wound dressing material, mainly due to its high content of macroelements such as potassium (supports the maintenance of adequate moisture levels in the wound), calcium (involved in hemostasis and tissue regeneration) and magnesium (essential for protein synthesis and cell proliferation). In addition, iron (247 mg kg^{-1}) and zinc (68 mg kg^{-1}) promote tissue regeneration and have an anti-inflammatory effect, accelerating the healing process.

Table 1 Contents of selected elements on a dry weight basis

Element	Method	Unit	Mean	Confidence interval	Standard deviation (α = 0.05)
K	FAAS	g kg^{-1}	28.3	0.3	0.2
Ca	FAAS	g kg^{-1}	22.0	0.6	0.6
Mg	FAAS	g kg^{-1}	9.72	0.17	0.16
Mn	FAAS	mg kg^{-1}	308	7	6
Fe	FAAS	mg kg^{-1}	247	14	13
Zn	FAAS	mg kg^{-1}	68	3	3
Na	FAAS	mg kg^{-1}	63	6	6
Cu	FAAS	mg kg^{-1}	13.7	0.7	0.7
Co	ICP	µg kg^{-1}	145	11	10
Cr	ICP	µg kg^{-1}	120	4	4

Physicochemical properties of the CS/Kef/WE and CS/Kef/EE

Owing to the growing need for new, effective, and environmentally friendly wound dressing materials, we obtained chitosan–kefiran films with two *Hen* extracts: ethanol (CS/Kef/EE) and water (CS/Kef/WE). The obtained degree of cross-linking of CS/Kef, CS/Kef/WE, and CS/Kef/EE was 58%, 59%, and 61%, respectively.

The chemical structure of the materials was confirmed by ATR-FTIR analysis (Fig. 2a). On the CS/Kef film spectrum, a band around 3293 cm^{-1} is associated with the vibration of hydroxyl groups present in chitosan[58,59] and the kefiran components.[60,61] The band at 2931 cm^{-1} is associated with symmetric and asymmetric C–H vibrations. Moreover, a band at 1640 cm^{-1} is present on the spectrum, attributed to C═O amide groups, while an amide II band appears at 1554 cm^{-1}. The bands at 1260 cm^{-1} and 1156 cm^{-1} can be attributed to asymmetric C–O–C stretching, and the peaks at 1065 cm^{-1} and 1025 cm^{-1} are due to C–O stretching.[60] On the spectrum of CS/Kef/WE and CS/Kef/EE films, bands from chitosan and kefiran are present (3358 cm^{-1}, 1637 cm^{-1}, 1583 cm^{-1}, 1261 cm^{-1}, 1153 cm^{-1}, 1070 cm^{-1}, 1029 cm^{-1} for CS/Kef/WE and 3293 cm^{-1}, 1267 cm^{-1}, 1089 cm^{-1}, 1047 cm^{-1} for CS/Kef/WE), as well as confirming the presence of *Hen* extract. Bands around 3010 cm^{-1} are attributed to CH stretching of the benzene rings of cannabinoids contained in the extracts. The two bands at around 2925 cm^{-1} and 2855 cm^{-1} stretch vibrations of the CH_3 and CH_2 groups of cannabinoids and fatty acid hydrocarbons.[62,63] Also present in the CS/Kef/WE spectrum is a distinct band at 1745 cm^{-1}, associated with vibrations of the benzene skeleton. The absence of some bands, as well as slight shifts on the spectrum of the CS/Kef/EE film, may be due to the presence of ethanol, which can affect the structure of chitosan,

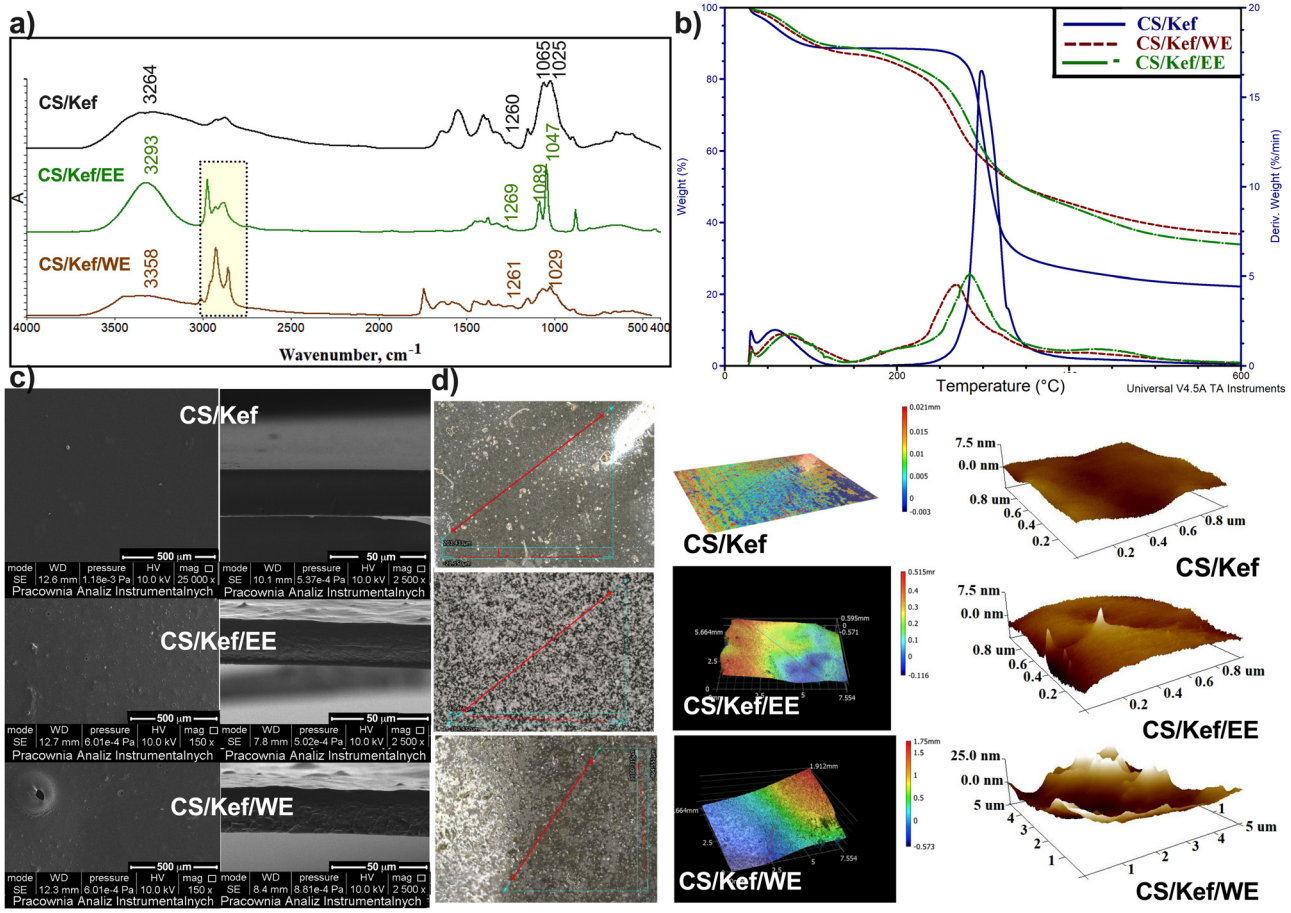

Fig. 2 Physicochemical properties of the obtained films. (a) ATR-FTIR spectra, (b) thermal analysis, (c) SEM images, and (d) AFM and profile images.

reducing the ability to form hydrogen bonds, thus affecting the visibility of these bands.

Thermal analysis is essential for evaluating the thermal stability of wound dressing materials, ensuring that they maintain their properties at different temperatures. The thermogravimetric analysis results are shown in Fig. 2b and Table S1 (ESI†). The decomposition of the CS/Kef film occurs in two stages The first stage, associated with water evaporation, shows 11% weight loss. In contrast, the second stage, associated with the principal degradation of polysaccharides, occurs with 67% weight loss. The decomposition of films with *Hen* extracts occurs in three stages. The first stage of CS/Kef/WE film degradation with a 13% mass loss includes removing extract-bound water and some polysaccharide decomposition. In the second stage (with a T_{max} of 268 °C and a mass loss of 40%), the main decomposition of chitosan and kefiran takes place, as well as some of the compounds in the hemp aqueous extract that decompose at lower temperatures (such as terpenes, or flavonoids[64]). The third stage (with a T_{max} of 422 °C and a loss of 10%) involves the further decomposition of residual polysaccharides and other substances in the extract that are more resistant to high temperatures. On the other hand, the second stage of CS/Kef/EE decomposition indicates the decomposition of polysaccharides and compounds in the ethanol extract (the more stable terpenes and parts of the cannabinoids, which begin to decompose at higher temperatures[65,66]), with a T_{max} higher than that of the aqueous extract, which may suggest that the ethanol extract is less likely to decompose at lower temperatures. In addition, the higher residue at 600 °C for films enriched with *Hen* extracts indicates better resistance to thermal decomposition of these materials, which may affect their durability as wound dressing materials, providing better stability under different conditions.

SEM analysis was used to describe the surface topography and cross-section of the materials to study the structure of the films (Fig. 2c). As can be seen, the surface and cross-section morphology of the CS/Kef film was relatively smooth and homogeneous, which is consistent with literature reports.[60,67] Adding *Hen* extract led to a rough surface and reduced the homogeneity and smoothness of the surface and cross-section of the film. It can be noted that fewer aggregates are observed in the CS/Kef/EE film compared to the CS/Kef/WE film. This may be related to the properties of ethanol, which better dissolves the active ingredients contained in hemp, promoting a more uniform distribution of these ingredients in the polysaccharide matrix.

AFM and profile analysis (Fig. 2d and Table 2) were used to investigate the surface topography and roughness differences

in more detail, which confirmed the SEM analysis's conclusions. The CS/Kef film shows a relatively smooth surface morphology with slight changes in height, confirming the absence of additives that change the structure. Adding *Hen* hemp extract increased the roughness parameters, and the type of solvent affected the values. Higher parameters were obtained for CS/Kef/WE. In this case, the surface is rougher, with pronounced irregularities and more significant changes in height, reflecting the presence of insoluble components, or aggregates, contained in the *Hen*. On the other hand, the surface of the CS/Kef/EE film is less rough, with mild changes in height. In general, roughness values should be optimal. A surface that is too smooth may not promote adequate cell adhesion and gas exchange, while a surface that is too rough may cause irritation or wound adhesion to the dressing. It was also reported that the cellular response to roughness varies by cell type.[68,69] Nevertheless, the roughness values obtained correspond with those obtained by other authors[70–72] and are suitable for wound dressing materials.

Contact angle measurements and the calculated surface free energy values are crucial in assessing the polar nature of potential wound dressing materials. They provide information about the ability of materials to interact with body fluids. As can be seen in Table 2, the CS/Kef film has a glycerin contact angle of 91°, indicating that the material is highly hydrophobic. Adding *Hen* extracts reduces this value significantly, suggesting a more hydrophilic nature of the materials. However, CS/Kef/WE has the most hydrophilic character, which is also confirmed by the polar component. The aqueous extract introduces more functional groups that can form hydrogen bonds, which increases the ability to absorb liquids. This makes such a film more suitable for exudative wounds, absorbing excess fluids from the wound well and preventing them from accumulating. On the other hand, the polar component of the CS/Kef/EE film is higher than that of CS/Kef but lower than that of CS/Kef/WE. Ethanol often introduces fewer polar components to the film's surface as a solvent, which may lower its ability to interact with water but slightly increase dispersion interactions. This means the material could be used when moderate moisture protection is needed, and the wound needs some fluid absorption capacity. Some authors have also observed the highly hydrophobic nature of the materials, using them in wound care or other areas of tissue engineering.[73,74] The obtained results correlate with the AFM outcomes. The CS/Kef/EE film showed less roughness, thus exhibiting a higher contact angle. Smoother surfaces reduce the contact points between the liquid droplet and the surface, increasing hydrophobicity.

Mechanical properties

Wound dressing materials should maintain structural integrity during application. Otherwise, even a tiny amount of tension near the wound can cause the dressings to break.[75] Therefore, the mechanical properties of the obtained materials were tested, and the results are shown in Table 3. The tensile strength of CS/Kef films is 25.15 ± 1.21 MPa while adding extracts increased this value. The highest tensile strength value was obtained for CS/Kef/WE. However, the difference in strength between aqueous and ethanol extract is slight. Notably, the film enriched with ethanol extract exhibited the highest elongation value among the tested samples. This may be due to the presence of hydrophobic compounds in the extract, which can act as plasticizers, increasing the flexibility and mobility of the polymer chains. The opposite correlation was observed for Young's modulus results. The CS/Kef/EE film showed a lower Young's modulus parameter than the CS/Kef/WE film, which was related to the presence of hydrophilic groups in the aqueous extract. This phenomenon was also confirmed by analysis of the surface free energy's contact angle measurements and polar and dispersive components. It is important to emphasize that an optimal wound dressing should exhibit softness and flexibility, with neither a high modulus nor excessive tensile strength. Based on this, it can be said that the obtained materials could be used as potential dressing materials.

Many reports in the literature confirm that adding extracts affects mechanical properties.[76–78] In the work of Nxumalo,[79] who studied chitosan films with *Lippia javanica*, *Syzygium cordatum*, and *Ximenia caffra* extracts, it was observed that adding extracts reduced tensile strength. The highest tensile strength in this case (23.4 MPa) was observed in films containing only chitosan. In another study, increasing the concentration of Cashew nut test a extract from 0 to 3% in the chitosan substrate led to a gradual increase in the material's tensile strength from 23.28 ± 0.74 to 28.63 ± 1.63 MPa.[80] In both cases, lower values were obtained than for the materials described in this work.

Table 2 Surface characterization of the obtained materials

	Roughness parameters [nm]			Average contact angle [θ, °] Measuring liquid		Surface free energy [mJ m^{-2}]		
Sample	R_q	R_a	R_{max}	Glycerin	Diiodomethane	γ_s	γ_s^d	γ_s^p
CS/Kef	0.911	0.749	5.58	91.91 ± 1.35	62.05 ± 1.03	26.61	25.53	1.09
CS/Kef/EE	1.15[a]	0.842[a]	14.2[a]	83.61 ± 1.25[a]	58.27 ± 1.27[a]	29.41[a]	26.40[a]	3.02[a]
CS/Kef/WE	10.9[a,b]	8.95[a,b]	61.5[a,b]	79.63 ± 1.70[a]	53.83 ± 0.86[a,b]	31.99[a]	28.18[a,b]	3.80[a,b]

The letters a, b, c indicate a statistically significant difference $p < 0.05$ when compared to the respective CS/Kef, CS/Kef/EE, and CS/Kef/WE. Three repetitions were performed to analyze roughness parameters. For the analysis of the contact angle and the surface free energy calculated from it, 10 repetitions were performed.

Table 3 The properties determined for the obtained materials

Sample	Mechanical properties			Oxygen permeability [mg mL^{-1}]	VWTR [g m^{-2} day^{-1}]
	Tensile strength (MPa)	Elongation (%)	Young's modulus (MPa)		
CS/Kef	25.15 ± 1.21	8.8 ± 0.12	123 ± 0.98	8.90 ± 0.09	1946 ± 0.19
CS/Kef/EE	34.81 ± 0.46[a]	10.73 ± 0.23[a]	119.3 ± 1.12[a]	10.11 ± 0.05[a]	2036 ± 1.28[a]
CS/Kef/WE	36.03 ± 0.23[a]	9.98 ± 0.86[a]	103 ± 1.43[a,b]	9.65 ± 0.13[a,b]	2143 ± 1.44[a,b]

The letters a, b, c indicate a statistically significant difference $p < 0.05$ when compared to the respective CS/Kef, CS/Kef/EE, and CS/Kef/WE. Three replicates were performed for each analysis.

Oxygen permeability

Oxygen permeability is a crucial parameter in wound dressing materials. These values should be high enough to ensure sufficient oxygen flow to the wound, promoting regenerative processes and preventing the growth of anaerobic bacteria.[81,82] Generally, dissolved oxygen in purified water is 7.0 to 14.6 mg L^{-1} (from 0 °C to 30 °C).[83] Low penetration of oxygen concentration into the wound bed reduces the tissue regeneration process or allows anaerobic bacteria to proliferate. According to the results, the negative control had a dissolved oxygen value of 7.56 mg L^{-1}, and the positive control had a dissolved oxygen value of 12.02 mg L^{-1}. As shown in Table 3, the CS/Kef film showed the lowest oxygen permeability value, while adding hemp extract improved this parameter. The CS/Kef/WE film showed the highest dissolved oxygen value, related to the presence of hydrophilic groups in the aqueous hemp extract. Overall, the values obtained for both extract-enriched materials are satisfactory for wound treatment.

Many other papers indicate that adding extracts to the chitosan increases oxygen permeability. In our study, this value did not exceed 11 cm^3 m^{-2} day^{-1}, indicating better barrier properties than previously described films containing other plant extracts. For example, chitosan films with propolis extract showed higher oxygen permeability values (up to 24 cm^3 m^{-2} day^{-1}).[84] In another study, chitosan films with sage extract had an oxygen permeability of 15 cm^3 m^{-2} day^{-1}, while films with thyme extract reached a value of 18 cm^3 m^{-2} day^{-1}.[79]

The water vapor transmission rate (WVTR)

Water vapor transmission rate plays an essential role in wound healing, as it controls the hydration of the wound area. According to the literature, an ideal dressing material should have a WVTR value of 2000–2500 g m^{-2} day^{-1}.[85] A lower WVTR value can inhibit wound healing due to inefficient absorption of wound exudates. At the same time, a WVTR that is too high can lead to drying of the wound surface due to excessive fluid loss in the form of water vapor.[86,87] The WVTR of the blank sample was 2763.34 ± 0.12 g m^{-2} day^{-1}. The water vapor permeability of the Cs/Kef sample was relatively low, while the addition of hemp extracts improved this property (Table 3). As with oxygen permeability, higher values were obtained for the CS/Kef/WE film, which is related to the hydrophilic nature of the sample. Adding an aqueous extract can lead to higher VWTR values, as the hydration of the material increases its moisture-carrying capacity. The CS/Kef/EE film, on the other hand, showed lower water vapor permeability than CS/Kef/WE due to its higher stiffness and reduced moisture-carrying capacity. This can be useful when it is necessary to keep more moisture within the wound. However, both obtained materials enriched with hemp extract permeate water vapor at optimal levels, which is beneficial for wound healing. In other articles, increased WVTR was observed when plant extracts were added to the polysaccharide matrix.[88–90] This is probably because the extracts' compounds can increase the matrix's porosity and elasticity, promoting better moisture transport and improving the transport of excess water from the wound. However, values obtained in other works are much lower than those obtained in this study (for example, for chitosan combined with *Hypericum perforatum* extract, the WVTR ranged from 530–718 g m^{-2} day^{-1}). This may affect the effectiveness of the wound dressings.[91]

Swelling analysis

Proper maintenance of wound moisture is crucial to the healing process. Wound dressing materials with adequate swelling ability can control the moisture around the wound, which is essential both in the initial phase and in the long-term healing process. The swelling rate of the obtained materials was tested at pH 5.5 and 7.4 for 24 hours. Wound dressings that respond to changes in pH around the wound can help minimize potential side effects. The skin around an injury has a different pH than the wound itself, affecting the impact of the compounds in the wound dressing material. As shown in Fig. 3a, the value of the swelling rate for pH 5.5 is lower than for pH 7.4. Chitosan may undergo a protonation process in an acidic environment, decreasing its ability to absorb water and swell. In addition, at lower pH, changes in the ionization of the functional groups of chitosan and kefiran can affect intermolecular interactions in the material's structure.[92] Notably, incorporating plant extract enhanced the swelling properties of the resultant materials. Relatively higher swelling values after 24 h were obtained for the CS/Kef/WE film (1016.67 ± 28.11%), while 977.33 ± 26.35% was obtained for the CS/Kef/EE film. This is probably due to the chemical composition of the extracts and their interaction with the polymer matrix. Nevertheless, all films presented a higher swelling degree than the other works (such as chitosan films with *Cynara cardunculus* leaves[93]) and the commercially available dressing, Tegaderm™ (9% after 48 h).[94]

Biodegradation analysis

Biodegradation studies of wound dressing materials are essential for effective wound care. Using such a dressing on a wound can promote healing processes while eliminating the need for

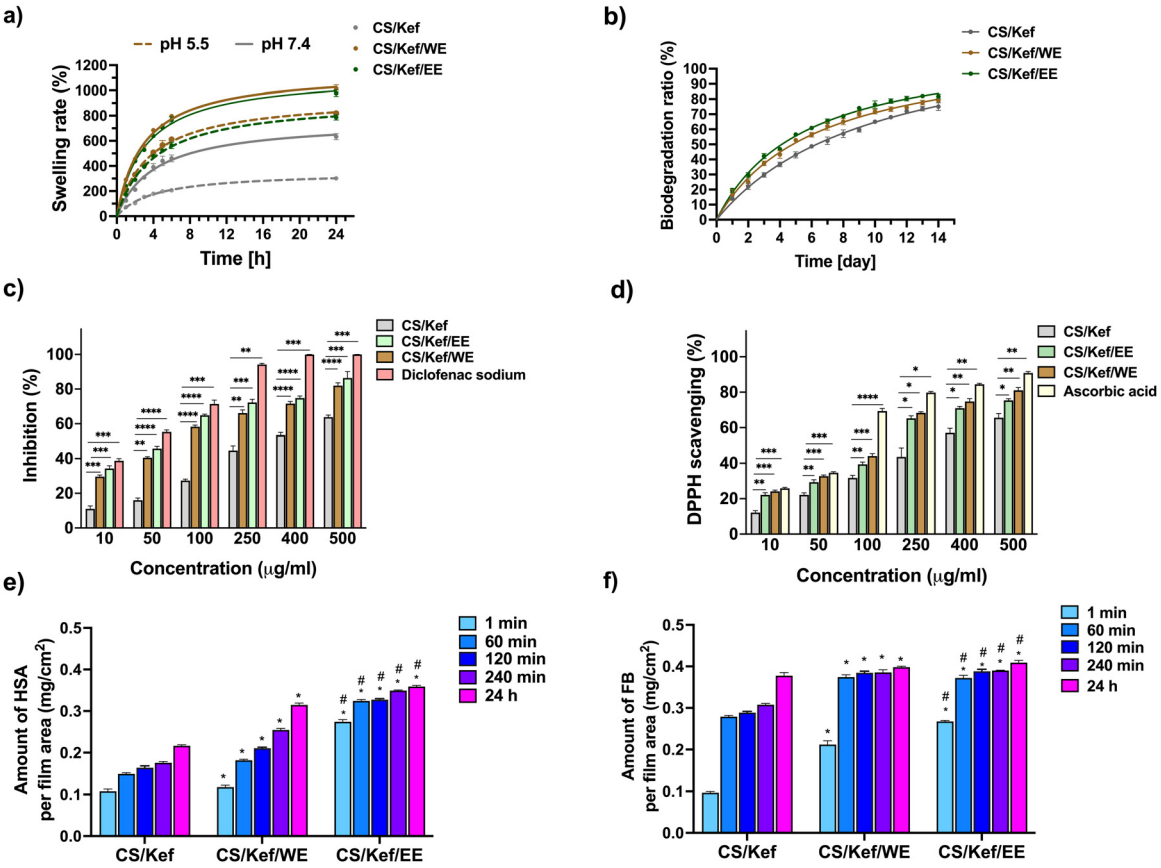

Fig. 3 Properties of the obtained films. (a) swelling rate in different pH, (b) biodegradation profile, (c) antioxidant properties, (d) anti-inflammatory properties, and (e) and (f) protein adsorption on the materials. $^{*, \#, \$}$ indicate $p < 0.05$ when compared to the corresponding CS/Kef and CS/Kef/WE, respectively.

frequent dressing changes and thus preventing secondary wound damage.[95] The degradation test of the designed materials was performed in a PBS solution containing hen (*Gallus domesticus*) egg white lysozyme, whose structure is very similar to the enzyme lysozyme in the human body. The test conditions (0.5 mg L^{-1} of lysozyme) were similar to the lysozyme concentration in typical exudate fluid from an inflamed wound.[96] As shown in Fig. 3b, all the obtained films are partially degraded, with the CS/Kef film without the extract degrading at 75 ± 2.65% after 14 days. *Hen* extract slightly improved the degree of degradation. However, the type of solvent in which the extracts were prepared did not significantly affect the values (79 ± 1.13% and 81 ± 1.53%) for (CS/Kef/WE and CS/Kef/EE, respectively). The slight differences may be due to the ethanol extract's better penetration and distribution of active compounds in the structure of the chitosan–kefiran film. It may lead to a more uniform presence of active ingredients, facilitating interaction with lysozyme and biodegradation processes. In addition, as shown in the antimicrobial study, the EE contains compounds with antimicrobial properties, which may result in more effective inhibition of bacterial degradation of the film structure. Lysozyme, an antimicrobial enzyme, may work more effectively in the presence of such compounds, thus accelerating biodegradation. Notably, the obtained materials biodegrade partially after only a short time. In contrast, the biodegradation of other materials described in the literature (such as chitosan–PVA–Basella alba extract composite) requires a longer time (after the 14th day, the % of weight loss was about 14%).[97] Thus, chitosan/kefiran films with the "Henola" extract may be a better alternative to other chitosan-based materials.

Anti-inflammatory properties

Research into anti-inflammatory properties is vital, as it influences the efficacy and performance of new wound dressing materials, enhances patient comfort, and promotes wound healing. We used a bovine serum protein denaturation test to study the anti-inflammatory properties of our materials. CS/Kef film without plant extract shows weak anti-inflammatory properties Fig. 3c. In contrast, CS/Kef/WE (81.93 ± 1.60%) and CS/Kef/EE (86.4 ± 3.67%) films have relatively strong anti-inflammatory properties. The differences in protein denaturation inhibition values between the CS/Kef/WE and CS/Kef/EE films are probably due to the composition of the extracts. Ethanol extract contains cannabinoids, terpenes, and other phytocannabinoids known for their anti-inflammatory properties. In addition, ethanol can better penetrate the chitosan–kefiran base material, enhancing its anti-inflammatory properties. However, the differences in anti-inflammatory

property values are insignificant, suggesting that both materials might be used in wound healing.

The anti-inflammatory potential of chitosan/kefiran-based material was superior to the *Ajuga integrifolia* extracts reported by Singh *et al.*[98] While the methanolic extract exhibited a maximum inhibition of BSA denaturation of approximately 40% at 500 μg mL^{-1}, our formulation demonstrated significantly higher inhibition at comparable concentrations. Slightly higher values of anti-inflammatory activity were observed for the material based on a mixture of chitosan and PVA enriched with *Basella alba* (81% at the highest concentration).[97] However, these are still lower values than for the CS/Kef/EE film. These results suggest that "Henola" extract has a beneficial effect on the anti-inflammatory properties of the films.

Antioxidant properties

Antioxidant properties are crucial in designing new wound dressing materials because they decrease or neutralize the impact of reactive oxygen species (ROS) and other oxidizing molecules. Wound and skin damage often increase oxidative stress, accelerating cellular aging and impeding healing. Antioxidants can help protect cells from oxidative damage.[99,100] We used the DPPH assay to study the antioxidant properties of the designed materials, and ascorbic acid was used as a model antioxidant compound. As shown in Fig. 3d, the CS/Kef film shows antioxidant properties of 65.6 ± 2.36% at the highest concentration. Adding *Hen* extract increased antioxidant properties; however, the type of solvent did not lead to significant differences in antioxidant properties at lower concentrations. A more significant difference was observed at a 500 μg mL^{-1} concentration, obtaining 75.4 ± 0.87% and 81.1 ± 1.53% using ethanol and water as a solvent, respectively. This difference may be due to interactions between the components present in the EE, which is causing a weakening of the ability to neutralize reactive oxygen species. In addition, papers in the literature confirm the antioxidant properties of the "Henola".[101] Many articles focus on studying the effects of plant extracts on chitosan materials. Bolgen *et al.*[102] developed a chitosan cryogel containing *Hypericum perforatum* oil. They determined its antioxidant activity using DPPH assays and found that the highest value of antioxidant activity was 69.99%. In another article,[103] the authors determined the antioxidant activity of microcapsules of chitosan-based red ginger oleoresin, obtaining a value of 61.99 ± 0.33%. This indicates that our films with the "Henola" extract show higher DPPH scavenging values. Consequently, these films could be applied to wound treatment.

Protein adsorption

Studying the interaction of biomaterials with proteins plays a significant role in the development of new materials for wound healing. When blood contacts foreign materials, plasma proteins first adsorb to their surface, further directing blood elements' adhesion. Our study examined the amount of bound protein after different incubation times. Human serum albumin (HSA) and fibrinogen (FB) were used as model proteins. HSA is the most abundant protein in blood plasma, while FB is directly related to blood clotting.[104,105] The results after selected incubation times are summarized in Fig. 3e and f, while the entire time range is given in Table S2 (ESI†). The results showed that the obtained films interact with both proteins, with relatively better results for fibrinogen adsorption. The surface of the obtained materials probably interacts better with specific chemical groups of fibrinogen, leading to stronger interactions.

The CS/Kef film interacts the weakest with HSA and FB, and adding each type of extract increased the amount of protein bound to the material. In the case of human serum albumin, the kind of extract was noticeably significant – more protein adsorbed to the surface of the material with the addition of the ethanol extract. In the case of fibrinogen, the differences in the amount of bound proteins between CS/Kef/WE and CS/Kef/EE films were slight. It may be due to the structure and properties of the obtained films, which make them effective in adsorbing proteins in a short time, and further incubations do not significantly affect the amount of bound protein. Notably, the bound protein values do not exceed 0.5 mg cm^{-2}, suggesting the potential suitability of the films for wound treatment applications. These data are consistent with the literature.[106,107] Low protein adsorption promotes a moist wound environment. It prevents the accumulation of proteins that can promote bacterial growth, reducing the risk of secondary infections.[108]

Antimicrobial test

The ideal wound dressing should not only act as a barrier against microorganisms but also possess antimicrobial properties to accelerate wound healing. The antimicrobial activity of the films obtained was studied on relevant wound infection bacteria – *Staphylococcus aureus*, *Pseudomonas aeruginosa*, and fungi – *Candida albicans*. Time-kill assays have shown that in the first hours of contact, obtained films reduced the viability of all tested microorganisms (Fig. 4a).

Our research demonstrated a significant reduction in the number of surviving *S. aureus* cells after adding the CS/Kef and CS/Kef/WE films. This reduction, observed within the first 4–8 hours, was followed by a slow recovery. Notably, the CS/Kef/EE film exhibited a robust inhibitory effect on the growth of *S. aureus*. At designated time intervals, the number of isolated cells was consistently 3.3 to 5.7 logs lower than the control sample and about 4 logs lower after 16 h and 20 h of incubation than the CS/Kef film. These results highlight the films' impressive effectiveness against these Gram-positive cocci and suggest a synergistic antimicrobial effect.

After the initial effect of obtained films on *P. aeruginosa*, the number of cells increased, and after 12 h (CS/Kef/WE, CS/Kef/EE) or 16 h (CS/Kef) of incubation, the recovery of the cells was comparable to that obtained from the control.

As shown in the figures, our findings reveal the high inhibitory efficiency of all tested films against *C. albicans*. The number of isolated cells during 24 hours of incubation was consistently lower than those isolated from the control sample. It did not significantly exceed the initial number of cells (5.9 log). This robust antifungal activity of the films provides reassurance about their potential in combating fungal infections.

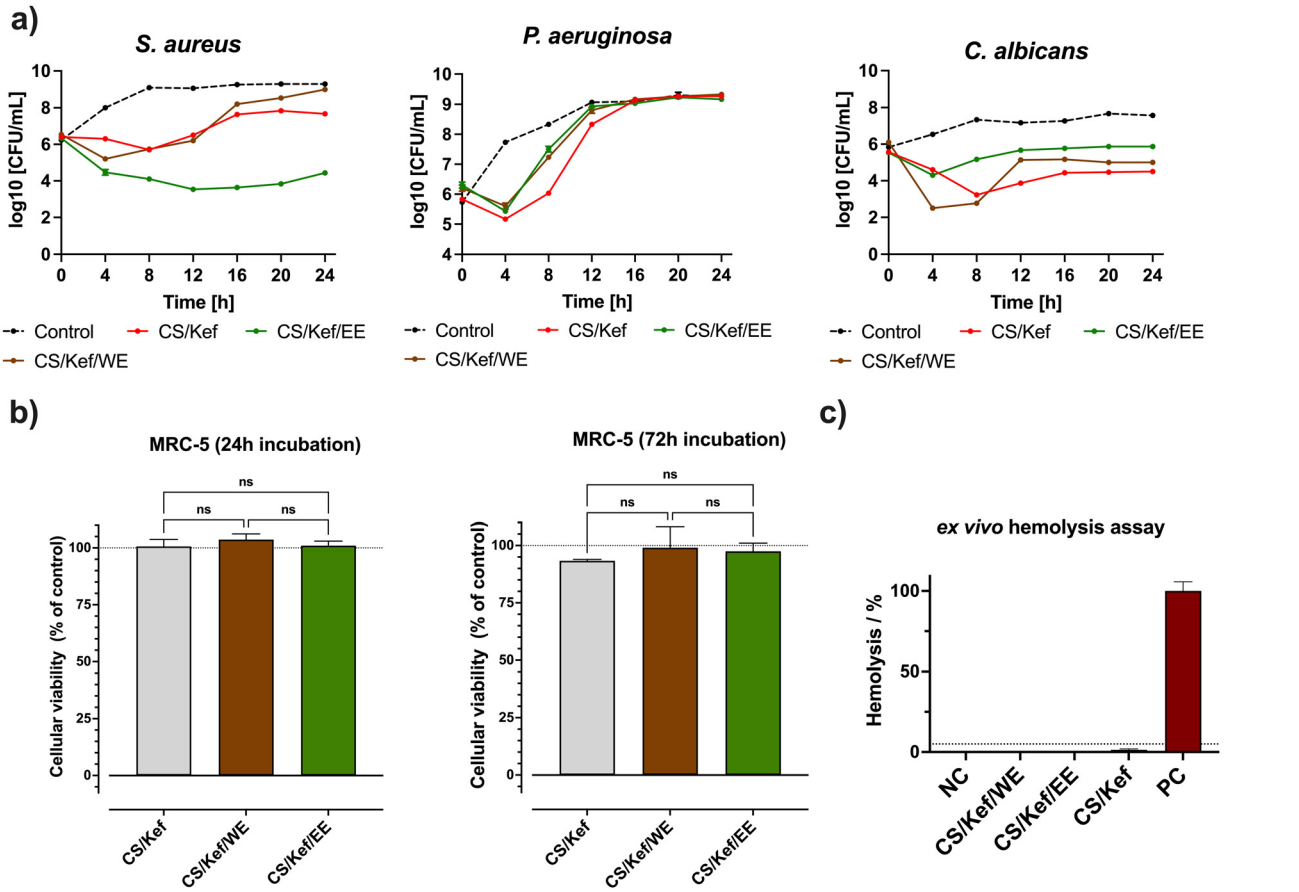

Fig. 4 Biological properties of the obtained films. (a) Antimicrobial properties against *S. aureus*, *P. aeruginosa*, and *C. albicans*, (b) cytotoxicity (n = 3, expressed as mean (SD)), and (c) hemolysis assay (n = 3, expressed as mean (SD)).

Several studies have demonstrated the antibacterial and antifungal activity of kefiran and chitosan.[109–114] These studies showed that chitosan and kefiran preparations could inhibit the growth of several Gram-positive and Gram-negative bacterial strains. However, the antimicrobial activity was more effective against Gram-positive. It agrees with our findings. The higher activity of chitosan against Gram-positive bacteria than Gram-negative may be due to their different cellular wall structure, which is the target point for chitosan. The antimicrobial activity of the chitosan is a result of the interaction of the cationic chitosans with anionic moieties at the cell surface, thereby altering cell permeability and consequent leakage of cell inclusions and forming a coating on its surface and thus preventing access to external nutrients, eventually leading to the death of the cell.[115]

Interestingly, the inhibitory activity of chitosan was found to be pH-dependent.[112] This may be why the obtained films possessed high activity against *C. albicans*, as the pH used for the antifungal activity assessment medium is lower than that of the antibacterial tests.

Biocompatibility of the films

Another essential feature of a beneficial wound dressing is its non-cytotoxicity. To evaluate the cytotoxicity of the obtained materials, the Alamar blue test was used after 24 h and 72 h on human fibroblasts (MRC-5), a widely recognized equivalent of human skin *in vitro* testing, fitting well with EU regulations encouraging the replacement of animal models (EU Directive 2010/63/EU).[116,117] The results showed that after 24 h incubation, the viability of MRC-5 cells on CS/Kef film did not decrease compared to the control (Fig. 4b). In contrast, adding the extract to the polysaccharide matrix resulted in a slight increase in cell viability. However, while differences in cell viability are noticeable (104 ± 2.52% for the CS/Kef/WE *versus* 101 ± 2.00% for the CS/Kef/EE), they are statistically insignificant. On the other hand, after 72 h of incubation, a significant decrease in cell viability is seen for the CS/Kef sample compared to 24 h of incubation. In contrast, the reduction in the different samples is insignificant (99 ± 3.59% for CS/Kef/WE and 97.5 ± 3.01% for CS/Kef/EE). ISO 10993-12: 2012[118] provides guidelines for the cytotoxicity testing of biomaterials. According to this standard, the obtained films were classified as non-toxic, confirming their suitability for application as wound dressing materials.

Moreover, the hemolysis test was conducted to further investigate the *ex vivo* blood biocompatibility. It is one of the most significant properties that should be assessed for any biomaterial intended to come into contact with blood to

prevent serious adverse effects in their applications.[119,120] As shown in Fig. 4c, deionized water (positive control) showed hemolysis, while the PBS (negative control) did not. The results with films showed that all the samples tested were non-hemolytic. The ISO 10993-4 standard precisely describes safe biomaterials as having a percentage of hemolysis $\leq 5\%$[121] and our materials exhibited negligible, and insignificant hemolysis of 1.37 ± 0.63%, 0.24 ± 0.13%, and 0.23 ± 0.15% for CS/Kef, CS/Kef/WE and CS/Kef/EE, respectively, compared to positive control.

Conclusions

In this study, we obtained films based on a mixture of chitosan and kefiran, which are crosslinked with the dialdehyde of kefiran. They were further enriched with aqueous or ethanolic extract of Hen to provide these materials with mainly antioxidant, anti-inflammatory, and antimicrobial properties. The results showed that the films were rough, flexible, and durable. The analysis of Hen's composition proved that the plant is rich in micronutrients, which probably positively affects tissue regeneration. It is worth noting that the type of solvent in the Hen extract affected some of the film's final properties. For example, the aqueous extract film showed higher cell viability (104 ± 2.52%) than the ethanolic extract (101 ± 2.00%).

On the other hand, the CS/Kef/EE film showed more potent anti-inflammatory properties (86.4 ± 3.67% at a concentration of 500 μg mL^{-1}) than CS/Kef/WE (81.93 ± 1.60%). In addition, the values of bound HSA and FB proteins on both materials do not exceed 0.5 mg cm^{-2}, suggesting the potential suitability of the films for wound healing applications. Both samples also show antioxidant properties (75.4 ± 0.87% and 81.1 ± 1.53% for CS/Kef/EE and CS/Kef/WE, respectively). Our materials showed negligible and insignificant hemolysis of 1.37 ± 0.63%, 0.24 ± 0.13%, and 0.23 ± 0.15% for CS/Kef, CS/Kef/WE, and CS/Kef/EE, respectively, compared to the positive control. Moreover, all tested films effectively inhibit the growth of *C. albicans* (preventing growth above 5.9 log), and the CS/Kef/EE film showed the most substantial effect against *S. aureus* (reduction of 3.3–5.7 log). In conclusion, the results showed that CS/Kef/WE and CS/Kef/EE films might be used as potential wound dressing materials for further research.

Author contributions

Dorota Chelminiak-Dudkiewicz: conceptualization, investigation, collection of the data, interpretation of data, funding acquisition, visualization, writing the original paper. Miloslav Machacek and Jolanta Dlugaszewska: investigation, partial interpretation of data. Aleksander Smolarkiewicz-Wyczachowski, Kinga Mylkie, Magdalena Kozlikova, and Sebastian Druzynski: investigation. Rafal Krygier: plant grower, preparation of the plant. Marta Ziegler-Borowska: revising the paper, supervising.

Data availability

Data are available upon request from the authors.

Conflicts of interest

There are no conflicts to declare.

Acknowledgements

This work was supported by the National Science Centre Poland grant UMO-2022/47/D/NZ7/01821 and partial by the Charles University SVV 260 664.

References

1 W. Liu, M. Wang, W. Cheng, W. Niu, M. Chen, M. Luo, C. Xie, T. Leng, L. Zhang and B. Lei, *Bioact. Mater.*, 2021, **6**, 721–728.
2 T. A. Harris-Tryon and E. A. Grice, *Science*, 2022, **376**, 940–945.
3 E. M. Tottoli, R. Dorati, I. Genta, E. Chiesa, S. Pisani and B. Conti, *Pharmaceutics*, 2020, **12**, 735.
4 D. Chelminiak-Dudkiewicz, M. Machacek, J. Dlugaszewska, M. Wujak, A. Smolarkiewicz-Wyczachowski, S. Bocian, K. Mylkie, T. Goslinski, M. P. Marszall and M. Ziegler-Borowska, *Int. J. Biol. Macromol.*, 2023, **253**, 126933.
5 K. Zhang, X. Jiao, L. Zhou, J. Wang, C. Wang, Y. Qin and Y. Wen, *Biomaterials*, 2021, **276**, 121040.
6 S. Nour, N. Baheiraei, R. Imani, M. Khodaei, A. Alizadeh, N. Rabiee and S. M. Moazzeni, *J. Mater. Sci.: Mater. Med.*, 2019, **30**, 120.
7 A. A. Alyamani, M. H. Al-Musawi, S. Albukhaty, G. M. Sulaiman, K. M. Ibrahim, E. M. Ahmed, M. S. Jabir, H. Al-Karagoly, A. A. Aljahmany and M. K. A. Mohammed, *Molecules*, 2023, **28**, 2501.
8 R. Zhang, B. Yu, Y. Tian, L. Pang, T. Xu, H. Cong and Y. Shen, *Appl. Mater. Today*, 2022, **26**, 101396.
9 F. Tao, Y. Cheng, X. Shi, H. Zheng, Y. Du, W. Xiang and H. Deng, *Carbohydr. Polym.*, 2020, **230**, 115658.
10 W. Peng, D. Li, K. Dai, Y. Wang, P. Song, H. Li, P. Tang, Z. Zhang, Z. Li, Y. Zhou and C. Zhou, *Int. J. Biol. Macromol.*, 2022, **208**, 400–408.
11 V. Hegde, U. T. Uthappa, T. Altalhi, H.-Y. Jung, S. S. Han and M. D. Kurkuri, *Mater. Today Commun.*, 2022, **33**, 104813.
12 K. M. Pasaribu, S. Ilyas, T. Tamrin, I. Radecka, S. Swingler, A. Gupta, A. G. Stamboulis and S. Gea, *Int. J. Biol. Macromol.*, 2023, **230**, 123118.
13 A. Moeini, P. Pedram, P. Makvandi, M. Malinconico and G. Gomez d'Ayala, *Carbohydr. Polym.*, 2020, **233**, 115839.
14 D. Chelminiak-Dudkiewicz, M. Wujak, D. T. Mlynarczyk, J. Dlugaszewska, K. Mylkie, A. Smolarkiewicz-Wyczachowski and M. Ziegler-Borowska, *Heliyon*, 2024, **10**, e35389.

15 Z. Zakaria, M. S. Islam, A. Hassan, M. K. Mohamad Haafiz, R. Arjmandi, I. M. Inuwa and M. Hasan, *Adv. Mater. Sci. Eng.*, 2013, **2013**, 629092.
16 F. Seidi, M. Khodadadi Yazdi, M. Jouyandeh, M. Dominic, H. Naeim, M. N. Nezhad, B. Bagheri, S. Habibzadeh, P. Zarrintaj, M. R. Saeb and M. Mozafari, *Int. J. Biol. Macromol.*, 2021, **183**, 1818–1850.
17 R. Adamski and D. Siuta, *Molecules*, 2021, **26**, 1976.
18 B. Shi, Z. Hao, Y. Du, M. Jia and S. Xie, *BioResources*, 2024, **19**, 4001.
19 EP4385528A1, 2023.
20 J. M. R. Tingirikari, A. Sharma and H.-J. Lee, *J. Ethnic Foods*, 2024, **11**, 35.
21 S. M. John and S. Deeseenthum, *Songklanakarin J. Sci. Technol.*, 2015, **37**, 275–282.
22 F. Mehrali, H. Ziyadi, M. Hekmati, R. Faridi-Majidi and M. Qomi, *SN Appl. Sci.*, 2020, **2**, 895.
23 H. Radhouani, S. Correia, C. Gonçalves, R. L. Reis and J. M. Oliveira, *Polymers*, 2021, **13**, 1342.
24 F. Doustdar, A. Olad and M. Ghorbani, *Int. J. Biol. Macromol.*, 2022, **208**, 912–924.
25 V. A. Reyna-Urrutia, V. Mata-Haro, J. V. Cauich-Rodriguez, W. A. Herrera-Kao and J. M. Cervantes-Uc, *Eur. Polym. J.*, 2019, **117**, 424–433.
26 M. Goudarzi, H. Kalantari and M. Rezaei, *Hum. Exp. Toxicol.*, 2018, **37**, 532–539.
27 K. Výborný, J. Vallová, Z. Kočí, K. Kekulová, K. Jiráková, P. Jendelová, J. Hodan and Š. Kubinová, *Sci. Rep.*, 2019, **9**, 10674.
28 D. Scheffel, L. Bianchi, D. Soares, F. Basso, C. Sabatini, C. de Souza Costa, D. Pashley and J. Hebling, *Operative Dentistry*, 2015, **40**, 44–54.
29 M. Hajialyani, D. Tewari, E. Sobarzo-Sánchez, S. M. Nabavi, M. H. Farzaei and M. Abdollahi, *Int. J. Nanomed.*, 2018, **13**, 5023–5043.
30 B. Gorain, M. Pandey, N. H. Leng, C. W. Yan, K. W. Nie, S. J. Kaur, V. Marshall, S. P. Sisinthy, J. Panneerselvam, N. Molugulu, P. Kesharwani and H. Choudhury, *Int. J. Pharm.*, 2022, **617**, 121617.
31 C. W. Kuo, Y. F. Chiu, M. H. Wu, M. H. Li, C. N. Wu, W. S. Chen and C. H. Huang, *Polymers*, 2021, **13**, 579.
32 K. Witkowska, M. Paczkowska-Walendowska, T. Plech, D. Szymanowska, B. Michniak-Kohn and J. Cielecka-Piontek, *Int. J. Mol. Sci.*, 2023, **24**, 17229.
33 C. Hemanth and S. Vimal, *Cureus*, 2024, **16**, e70103.
34 M. Saied, A. Ward and S. F. Hamieda, *Sci. Rep.*, 2024, **14**, 3430.
35 P. K. Monou, A. M. Mamaligka, E. K. Tzimtzimis, D. Tzetzis, S. Vergkizi-Nikolakaki, I. S. Vizirianakis, E. G. Andriotis, G. K. Eleftheriadis and D. G. Fatouros, *Pharmaceutics*, 2022, **14**, 1637.
36 COBORU, *Polish National List of Agricultural Plant Varieties*, 2021, **350**, 32–33.
37 M. Teleszko, A. Zając and T. Rusak, *Molecules*, 2022, **27**, 1448.
38 J. Frankowski, A. Wawro, J. Batog and H. Burczyk, *J. Nat. Fibers*, 2022, **19**, 7283–7295.
39 D. Gimeno-Martínez, M. Igual, P. García-Segovia, J. Martínez-Monzó and J. Navarro-Rocha, *Biol. Life Sci. Forum*, 2023, **26**, 89.
40 M. Teleszko, A. Zając and T. Rusak, *Molecules*, 2022, **27**, 1448.
41 A. Przybylska-Balcerek, J. Frankowski, M. Graczyk, G. Niedziela, D. Sieracka, S. Wacławek, T. H. Sázavská, M. Buśko, L. Szwajkowska-Michałek and K. Stuper-Szablewska, *Molecules*, 2024, **29**, 4178.
42 M. Teleszko, A. Zając and T. Rusak, *Molecules*, 2022, **27**, 1448.
43 J. A. Piermaria, A. Pinotti, M. A. Garcia and A. G. Abraham, *Food Hydrocolloids*, 2009, **23**, 684–690.
44 M. Ghasemlou, F. Khodaiyan, K. Jahanbin, S. M. T. Gharibzahedi and S. Taheri, *Food Chem.*, 2012, **133**, 383–389.
45 F. Karimi, Y. Hamidian, F. Behrouzifar, R. Mostafazadeh, A. Ghorbani-HasanSaraei, M. Alizadeh, S.-M. Mortazavi, M. Janbazi and P. Naderi Asrami, *Food Chem. Toxicol.*, 2022, **164**, 113053.
46 O. Carrier and D. Bonn, in *Droplet Wetting and Evaporation*, ed. D. Brutin, Academic Press, Oxford, 2015, pp. 15–23, DOI: 10.1016/B978-0-12-800722-8.00002-3.
47 Y. Liu, Z. Cai, L. Sheng, M. Ma, Q. Xu and Y. Jin, *Carbohydr. Polym.*, 2019, **215**, 348–357.
48 A. Nowak, M. Zagórska-Dziok, M. Perużyńska, K. Cybulska, E. Kucharska, P. Ossowicz-Rupniewska, K. Piotrowska, W. Duchnik, Ł. Kucharski, T. Sulikowski, M. Droździk and A. Klimowicz, *Front. Pharmacol.*, 2022, **13**, 896706.
49 D. Chelminiak-Dudkiewicz, A. Smolarkiewicz-Wyczachowski, K. Mylkie, M. Wujak, D. T. Mlynarczyk, P. Nowak, S. Bocian, T. Goslinski and M. Ziegler-Borowska, *Sci. Rep.*, 2022, **12**, 18658.
50 L. Marangoni Júnior, R. P. Vieira and C. A. R. Anjos, *Carbohydr. Polym.*, 2020, **246**, 116609.
51 S. M. A. S. Keshk, A. M. Ramadan, A. G. Al-Sehemi, E. S. Yousef and S. Bondock, *Carbohydr. Polym.*, 2016, **152**, 624–631.
52 S. K. Bajpai, M. Bajpai and F. F. Shah, *Designed Monomers Polym.*, 2016, **19**, 406–419.
53 K. Wegrzynowska-Drzymalska, P. Grebicka, D. T. Mlynarczyk, D. Chelminiak-Dudkiewicz, H. Kaczmarek, T. Goslinski and M. Ziegler-Borowska, *Materials*, 2020, **13**, 3413.
54 K. Wegrzynowska-Drzymalska, D. T. Mlynarczyk, D. Chelminiak-Dudkiewicz, H. Kaczmarek, T. Goslinski and M. Ziegler-Borowska, *Int. J. Mol. Sci.*, 2022, **23**, 9700.
55 X. Chen, A. Pizzi, B. Zhang, X. Zhou, E. Fredon, C. Gerardin and G. Du, *Wood Sci. Technol.*, 2022, **56**, 63–85.
56 H. Radhouani, C. Gonçalves, F. R. Maia, J. M. Oliveira and R. L. Reis, *J. Bioact. Compat. Polym.*, 2018, **33**, 461–478.
57 H. Lee, J. You, H.-J. Jin and H. W. Kwak, *Carbohydr. Polym.*, 2020, **232**, 115771.
58 M. H. R. Barbosa, S. D. Á. Gonçalves, L. Marangoni Júnior, R. M. V. Alves and R. P. Vieira, *J. Food Measure. Charact.*, 2022, **16**, 2011–2023.

59 D. Chełminiak-Dudkiewicz, A. Smolarkiewicz-Wyczachowski, M. Ziegler-Borowska and H. Kaczmarek, *J. Photochem. Photobiol., B*, 2024, **251**, 112850.
60 C. O. Marinho, T. C. Vianna, R. R. R. Cecci, L. Marangoni Júnior, R. M. V. Alves and R. P. Vieira, *Mater. Today Commun.*, 2022, **32**, 103902.
61 C. O. Marinho, L. Marangoni Júnior, R. R. R. Cecci and R. P. Vieira, *Coatings*, 2023, **13**, 465.
62 H. Li, Q.-S. Zhao, S.-L. Chang, T.-R. Chang, M.-H. Tan and B. Zhao, *J. Mol. Liq.*, 2022, **347**, 118318.
63 S. Suman, L. Loveleen, M. Bhandari, A. Syed, A. H. Bahkali, R. Manchanda and S. Nimesh, *Artif. Cells, Nanomed., Biotechnol.*, 2022, **50**, 343–351.
64 G. Mijas, M.-J. Lis, S. Pérez-Rentero, M. Riba-Moliner, M. Martí, D. Cayuela and A. Manich, *J. Wood Chem. Technol.*, 2022, **42**, 181–192.
65 L. Marrot, K. Meile, M. Zouari, D. DeVallance, A. Sandak and R. Herrera, *Molecules*, 2022, **27**, 2794.
66 G. Mijas, A. Manich, M.-J. Lis, M. Riba-Moliner, I. Algaba and D. Cayuela, *J. Wood Chem. Technol.*, 2021, **41**, 210–219.
67 H. Salmanian, F. Khodaiyan and S. S. Hosseini, *J. Food Bioprocess Eng.*, 2019, **2**, 101–106.
68 V. Sharma, N. Patel, N. Kohli, N. Ravindran, L. Hook, C. Mason and E. García-Gareta, *Biomed. Mater.*, 2016, **11**, 055001.
69 P. Agrawal and K. Pramanik, *Tissue Eng Regener. Med.*, 2016, **13**, 485–497.
70 M. Hajikhani, Z. Emam-Djomeh and G. Askari, *Int. J. Biol. Macromol.*, 2021, **172**, 143–153.
71 X. Fu, J. K. Wang, A. C. Ramírez-Pérez, C. Choong and G. Lisak, *Mater. Sci. Eng., C*, 2020, **108**, 110392.
72 H. Adeli, M. T. Khorasani and M. Parvazinia, *Int. J. Biol. Macromol.*, 2019, **122**, 238–254.
73 M. Shahrousvand, V. Haddadi-Asl and M. Shahrousvand, *Int. J. Biol. Macromol.*, 2021, **180**, 36–50.
74 G. W. Oh, S. C. Ko, J. Y. Je, Y. M. Kim, J. Oh and W. K. Jung, *Int. J. Biol. Macromol.*, 2016, **93**, 1549–1558.
75 T. T.-P. Ho, V. K. Doan, N. M.-P. Tran, L. K.-K. Nguyen, A. N.-M. Le, M. H. Ho, N.-T. Trinh, T. Van Vo, L. D. Tran and T.-H. Nguyen, *Mater. Sci. Eng., C*, 2021, **120**, 111724.
76 S. Rafieian, H. Mahdavi and M. E. Masoumi, *J. Ind. Text.*, 2021, **50**, 1456–1474.
77 M. Maizura, A. Fazilah, M. H. Norziah and A. A. Karim, *J. Food Sci.*, 2007, **72**, C324–C330.
78 P. Jenifer, M. Kalachaveedu, A. Viswanathan, A. Gnanamani and A. Mubeena, *J. Bioact. Compat. Polym.*, 2018, **33**, 612–628.
79 K. A. Nxumalo, O. A. Fawole and A. O. Aremu, *Processes*, 2024, **12**, 23.
80 T. T. Dang, L. A. T. Nguyen, D. T. Dau, Q. S. Nguyen, T. N. Le and T. Q. N. Nguyen, *R. Soc. Open Sci.*, 2024, **11**, 241236.
81 A. Hautmann, D. Kedilaya, S. Stojanović, M. Radenković, C. K. Marx, S. Najman, M. Pietzsch, J. F. Mano and T. Groth, *Biomater. Adv.*, 2022, **142**, 213166.
82 H. Derakhshandeh, S. S. Kashaf, F. Aghabaglou, I. O. Ghanavati and A. Tamayol, *Trends Biotechnol.*, 2018, **36**, 1259–1274.
83 M. Shafique, M. Sohail, M. U. Minhas, T. Khaliq, M. Kousar, S. Khan, Z. Hussain, A. Mahmood, M. Abbasi, H. C. Aziz and S. A. Shah, *Int. J. Biol. Macromol.*, 2021, **170**, 207–221.
84 K. Stanicka, R. Dobrucka, M. Woźniak, A. Sip, J. Majka, W. Kozak and I. Ratajczak, *Polymers*, 2021, **13**, 3888.
85 M. T. Khorasani, A. Joorabloo, A. Moghaddam, H. Shamsi and Z. MansooriMoghadam, *Int. J. Biol. Macromol.*, 2018, **114**, 1203–1215.
86 Y. Han, J. Ding, J. Zhang, Q. Li, H. Yang, T. Sun and H. Li, *Int. J. Biol. Macromol.*, 2021, **184**, 739–749.
87 H. Gharib Khajeh, M. Sabzi, S. Ramezani, A. A. Jalili and M. Ghorbani, *Colloids Surf., A*, 2022, **633**, 127891.
88 S. Güneş and F. Tıhmınlıoğlu, *Int. J. Biol. Macromol.*, 2017, **102**, 933–943.
89 T. N. T. Tran, N. H.-T. Le and Q. M. Tran, *Int. J. Biol. Macromol.*, 2024, **271**, 132531.
90 S. Fahimirad, P. Satei, A. Ganji and H. Abtahi, *J. Drug Delivery Sci. Technol.*, 2023, **87**, 104734.
91 E. Arıöz, S. B. Ay and D. Erkmen, *J. Eng. Basic Sci.*, 2024, **2**, 1–7.
92 K. Ngece, B. A. Aderibigbe, D. T. Ndinteh, Y. T. Fonkui and P. Kumar, *Int. J. Biol. Macromol.*, 2021, **172**, 350–359.
93 T. Brás, D. Rosa, A. C. Gonçalves, A. C. Gomes, V. D. Alves, J. G. Crespo, M. F. Duarte and L. A. Neves, *Int. J. Biol. Macromol.*, 2020, **163**, 1707–1718.
94 A. Zhang, L. Yang, Y. Lin, H. Lu, Y. Qiu and Y. Su, *J. Biomater. Sci., Polym. Ed.*, 2013, **24**, 1883–1899.
95 P. Deng, W. Jin, Z. Liu, M. Gao and J. Zhou, *Carbohydr. Polym.*, 2021, **260**, 117767.
96 K. G. Dilruba Öznur and T. D. Ay. şe Pınar, *Polym. Bull.*, 2024, **81**, 1563–1596.
97 O. J. D'Souza, T. Gasti, V. D. Hiremani, J. P. Pinto, S. S. Contractor, A. K. Shettar, D. Olivia, S. B. Arakera, S. P. Masti and R. B. Chougale, *Int. J. Biol. Macromol.*, 2023, **225**, 673–686.
98 H. Singh, S. Kumar and A. Arya, *Sci. Rep.*, 2024, **14**, 16754.
99 S. Xiong, R. Li, S. Ye, P. Ni, J. Shan, T. Yuan, J. Liang, Y. Fan and X. Zhang, *Int. J. Biol. Macromol.*, 2022, **220**, 109–116.
100 Q. Wei, K. Chen, X. Zhang, G. Ma, W. Zhang and Z. Hu, *Colloids Surf., B*, 2022, **209**, 112208.
101 A. Stasiłowicz-Krzemień, S. Sip, P. Szulc and J. Cielecka-Piontek, *Antioxidants*, 2023, **12**, 1390.
102 N. Bölgen, D. Demir, M. S. Yalçın and S. Özdemir, *Int. J. Biol. Macromol.*, 2020, **161**, 1581–1590.
103 J. Jayanudin, M. Fahrurrozi, S. K. Wirawan and R. Rochmadi, *Sustainable Chem. Pharm.*, 2019, **12**, 100132.
104 B. Singh and A. Dhiman, *Ind. Eng. Chem. Res.*, 2016, **55**, 9176–9188.
105 B. Yang, Y. Chen, Z. Li, P. Tang, Y. Tang, Y. Zhang, X. Nie, C. Fang, X. Li and H. Zhang, *Mater. Sci. Eng., C*, 2020, **110**, 110718.
106 H. P. Felgueiras, J. C. Antunes, M. C. L. Martins and M. A. Barbosa, in *Peptides and Proteins as Biomaterials for Tissue Regeneration and Repair*, ed. M. A. Barbosa and

M. C. L. Martins, Woodhead Publishing, 2018, pp. 1–27, DOI: 10.1016/B978-0-08-100803-4.00001-2.

107 D. Stan, E. Codrici, A.-M. Enciu, E. Olewnik-Kruszkowska, G. Gavril, L. L. Ruta, C. Moldovan, O. Brincoveanu, L.-A. Bocancia-Mateescu, A.-C. Mirica, D. Stan and C. Tanase, *Gels*, 2023, **9**, 476.

108 T. R. Kyriakides, in *Host Response to Biomaterials*, ed. S. F. Badylak, Academic Press, Oxford, 2015, pp. 81–116, DOI: 10.1016/B978-0-12-800196-7.00005-0.

109 A. Machul, D. Mikołajczyk, A. Regiel-Futyra, P. B. Heczko, M. Strus, M. Arruebo, G. Stochel and A. Kyzioł, *J. Biomater. Appl.*, 2015, **30**, 269–278.

110 D. Ailincai, L. Marin, S. Morariu, M. Mares, A.-C. Bostanaru, M. Pinteala, B. C. Simionescu and M. Barboiu, *Carbohydr. Polym.*, 2016, **152**, 306–316.

111 M. Ignatova, K. Starbova, N. Markova, N. Manolova and I. Rashkov, *Carbohydr. Res.*, 2006, **341**, 2098–2107.

112 M. Ganan, S. B. Lorentzen, J. W. Agger, C. A. Heyward, O. Bakke, S. H. Knutsen, B. B. Aam, V. G. H. Eijsink, P. Gaustad and M. Sørlie, *PLoS One*, 2019, **14**, e0210208.

113 K. Divya, S. Vijayan, T. K. George and M. S. Jisha, *Fibers Polym.*, 2017, **18**, 221–230.

114 K. L. Rodrigues, L. R. G. Caputo, J. C. T. Carvalho, J. Evangelista and J. M. Schneedorf, *Int. J. Antimicrob. Agents*, 2005, **25**, 404–408.

115 M. B. Kaczmarek, K. Struszczyk-Swita, X. Li, M. Szczęsna-Antczak and M. Daroch, *Front. Bioeng. Biotechnol.*, 2019, **7**, 243.

116 M. di Luca, M. Curcio, E. Valli, G. Cirillo, F. Voli, M. E. Butini, A. Farfalla, E. Pantuso, A. Leggio, F. P. Nicoletta, A. Tavanti, F. Iemma and O. Vittorio, *J. Mater. Chem. B*, 2019, **7**, 4361–4370.

117 C. M. A. Reijnders, A. van Lier, S. Roffel, D. Kramer, R. J. Scheper and S. Gibbs, *Tissue Eng., Part A*, 2015, **21**, 2448–2459.

118 M. Mirhaj, M. Tavakoli, J. Varshosaz, S. Labbaf, S. Salehi, A. Talebi, N. Kazemi, V. Haghighi and M. Alizadeh, *Carbohydr. Polym.*, 2022, **292**, 119648.

119 D. S. Ghataty, R. I. Amer, M. A. Amer, M. F. Abdel Rahman and R. N. Shamma, *Pharmaceutics*, 2023, **15**, 234.

120 M. S. Salami, G. Bahrami, E. Arkan, Z. Izadi, S. Miraghaee and H. Samadian, *BMC Complementary Med. Ther.*, 2021, **21**, 111.

121 F. Cui, J. Sun, J. Ji, X. Yang, K. Wei, H. Xu, Q. Gu, Y. Zhang and X. Sun, *J. Hazard. Mater.*, 2021, **406**, 124330.